LAPPEENRANTA UNIVERSITY OF TECHNOLOGY
LUT School of Engineering Science
Double Degree Programme in Chemical and Process Engineering

Kavun Vitalii

UNIFIED DESIGN OF CHROMATOGRAPHIC SEPARATION PROCESSES IN NON-IDEAL CONDITIONS – INFLUENCE OF NTP ON THE SHAPE AND POSITION OF THE FEASIBLE OPERATING PARAMETER SPACE

Examiners: Professor Tuomo Sainio
D.Sc. Jari Heinonen

ABSTRACT

Lappeenranta University of Technology
LUT School of Engineering Science
Double Degree Programme in Chemical and Process Engineering

Kavun Vitalii

Unified Design of chromatographic separation processes in non-ideal conditions – influence of NTP on the shape and position of the feasible operating parameter space

Master's Thesis

2016

73 pages, 41 figures, 14 tables and 1 appendix

Examiners: Professor Tuomo Sainio
D.Sc. Jari Heinonen

Keywords: Unified Design, triangle theory, number of theoretical plates, batch chromatography, steady state recycling

The investigation of the influence of the number of theoretical plates (NTP) on the region of feasible operating parameters was carried out by conducting a set of simulations with using special software MATLAB.

One part of modelling was devoted to batch chromatography separation of glucose and fructose under non-ideal conditions. To obtain the feasible operating region for this process the Unified Design method was applied. The key parameters of this method were calculated and boundaries of complete separation regions were found. The simulations were performed for different purity requirements (80%, 90% and 99.9%) and with different column efficiency. It was established that at certain (or minimum required value) NTP the operating boundaries at non-ideal conditions is close to be described by the boundaries of the region under ideal conditions. In order to verify it the additional simulations were done with different isotherm parameters for glucose and fructose. The one Henry constants were taken from the literature (for Dowex Monosphere 99/Ca gel type resin), another - were derived for the experimental column in the LUT laboratory, which was packed with Finex CS11GC gel type resin in Ca^{2+} form. The minimum number of theoretical plates was obtained for each purity constraints and type of the applied adsorbents. It was determined that for low requirements of the product purity the lower NTP is needed to use the operating parameters as for the separation region under ideal conditions.

Further study was devoted to SSR chromatography. The operating parameters obtained from batch simulations were used to design SSR, where showed its applicability. In addition, the productivity and eluent consumption of SSR were compared with batch chromatography.

ACKNOWLEDGEMENTS

I would like to express my deepest gratitude to my supervisor D.Sc. Jari Heinonen for his consultations, for being aware about the work progress and kept me active in research, contributing to the timely progress of the writing of the Master's thesis. I am deeply grateful to Professor Tuomo Sainio. I have learned a new in the field of theory of separation processes, including a new field for me – chromatography. Working with them was exciting, informative and interesting and I would not want to rest on laurels and continue to develop further in scientific sphere.

I wish to thank Liubov Lukina for providing a positive mood and support during the study at Lappeenranta University of Technology.

TABLE OF CONTENTS

LIST OF ABBREVIATIONS

EC	eluent consumption
FF	fresh feed
HETP	height of an equivalent theoretical plate
i.c.	ideal conditions
MTR	mass transfer resistance
NTP	number of theoretical plates
PR	productivity
PS–DVB	polystyrene-divinylbenzene
SAC	strong acid cation
SBA	strong base anion
SMB	simulated moving bed
SSR	steady state recycling
WAC	weak acid cation
WBA	weak base anion

INTRODUCTION

Over the past century the chromatography has evolved and it was found a lot of applications in analytical and in industrial scales, e.g., biotechnology, sugar, pharmaceutical fine chemical and other industries (Guiochon et al. 2006, 1-3).

Chromatography is a method of separation of several compounds. The separation is based on the component distribution in stationary phase and mobile phase. The components can be divided into the less and highly retained. The less retained component passes through the column faster (eluted firstly) while the movement of the highly retained component is lower because of the higher affinity for stationary phase (Wixom and Gehrke (ed.) 2010, 6).

Chromatography may be linear or nonlinear and performed under ideal or non-ideal conditions. When phase equilibrium concentrations of a solute in the stationary and mobile phases are proportional it is linear (at low concentrations), otherwise - nonlinear (at high concentrations). The ideal or non-ideal conditions mean ignoring axial dispersion and mass transfer resistance or not.

For different applications, chromatography can be divided into analytical and preparative. The first is used for determination of the concentration (or existence) of solutes in sample. It uses the much smaller columns with much smaller particles of solid phase compared with preparative scale. The latter is aimed to purify large amount of substance for production and selling purposes rather than analysis. The rate of production of highly pure products can be varied from milligram to thousand tons.

Batch chromatography is the most known and applied technique. To improve the productivity of the oldest separation process, the SSR (and its variations) and SMB chromatography were developed. There are many researches and scientific books, which describe in detail the processes and the equipment components.

SMB chromatography is the prospective technique for separation of binary mixtures. The implementation of the process occurs in many fields such as pharmaceutical applications, hydrocarbons separation and producing of high-fructose sugar. Nevertheless, the process designing is a great challenge. However, the simplified method was provided for designing

the SMB when the triangle theory was formulated. It is applied to obtain the operating conditions to reach a complete separation.

The further theory development allowed formulating of Unified Design for batch, SSR and SMB chromatography with using the same dimensionless operating parameters. It means, for example, that knowing the main operating parameters for batch process provides deriving the operating conditions for SMB in convenient way.

The aim of this research is devoted to find out the influence of the column efficiency on the feasible operating region. The batch chromatography of binary mixture (glucose and fructose) under non-ideal conditions is simulated in MATLAB software. The simulation requires the concentration of the components, the Henry constants and other process parameters. Based on the literature analysis, it is established that the appropriate adsorbent for considering sugar separation is strong acid cation (SAC) exchange resin in Ca^{2+} form and, for this reason, the Henry constants are found for Dowex Monosphere 99/Ca gel type resin and used in simulations. To obtain the operating region for this process with different column efficiency the Unified Design method is applied.

During the investigation, new targets were set. To ascertain in the received results, the new isotherm parameters are derived for experimental column, packed with Finex CS11GC SAC gel type resin in Ca^{2+} form, based on frontal analysis method. The comparison of the simulation results between discussed adsorbents is made. Further study is devoted to SSR chromatography. The transferring from batch to SSR process is done by Unified Design method. The additional simulations provided the comparison of productivity and eluent consumption between two separation processes.

1. LITERATURE REVIEW

1.1 Main parameters and performance indicators of preparative chromatography

During the optimization and design of the process of chromatographic separation, several main parameters should be considered.

1.1.1 Selectivity

Difficulty of the separation is indicated by a separation factor (or selectivity - α), which is characterizes chromatographic separation. It is a relative parameter. The selectivity depends on the mobile phase and material of stationary phase (Gottschalk (ed.) 2009, 225) and can be expressed by:

$$\alpha = \frac{q_j / c_j}{q_i / c_i} \tag{1.1}$$

where q and c are the concentrations in the adsorbent and in the mobile phase in of the solutes j and i, respectively.

The separation factor is always larger than or equal to unity ($\alpha \geq 1$). When the distribution coefficient quotient is equal to 1 no separation is possible. From 1 to 1.3 values – very difficult separation, 1.3-2.0 – appropriate separation, more than 2.0 – high tendency to separate.

The separation factor could be manipulated for achieving a suitable by substitution of solvent, stationary phase or by changing pH of mobile phase, temperature (The Theory of HPLC Chromatographic Parameters, 9).

1.1.2 Efficiency of Chromatographic Separations

For characterization of column efficiency in preparative chromatography the number of theoretical plates (NTP) N is used (Schmidt-Traub 2005, 51-54).

$$N = \frac{L_c}{HETP} \tag{1.2}$$

where L_c is the column length.

The HETP (height of an equivalent theoretical plate) as well as the NTP is the measure of the total band broadening, which consists the influence of the axial dispersion, which includes fluid dynamic non-idealities, and the mass transfer resistance. The plate height is characterized by the peak of Gaussian profile growth rate per unit length of considered column. Given the fact that peak profile is detected with time, the HETP can be calculated by Eq 1.3.

$$HETP = \left(\frac{\sigma_t}{t_R} \right)^2 L_c \tag{1.3}$$

where t_R is the retention time, σ_t is standard deviation of the peak.

In order to get the peak shape closer to the ideal rectangular elution profile and the peak width narrower, the higher efficiency column is needed. In real cases, due to mass transfer and hydrodynamic effects every peak has a certain, finite efficiency. The lower elution consumption, the narrower peak width and higher product concentration are the facts that give beneficial conditions for industrial scale chromatography.

In case when adsorbents with high efficiency are used and symmetrical peaks are achieved, NTP for component i can be calculated with the Gaussian distribution width w:

$$N_i = \left(\frac{t_R}{\sigma_t} \right)^2 = 16 \left(\frac{t_{R,i}}{w_i} \right)^2 = 5.55 \left(\frac{t_{R,i}}{w_{1/2,i}} \right)^2 \tag{1.4}$$

The efficiency per metre N_L can be derived from Eq. 1.5. This term is used for comparison of efficiencies of columns with different length.

$$N_L = \frac{N_i}{L} = \frac{1}{HETP} \tag{1.5}$$

The total column efficiency depends on the different mass transfer parameters and this influence is presented on Fig. 1.1. The x-axis of the plot corresponds to the interstitial velocity (or mobile phase velocity) and y-axis is the efficiency expressed by HETP. The van Deemter equation (Eq. 1.6) describes the curve of their dependence.

$$HETP = A + \frac{B}{u} + Cu \tag{1.6}$$

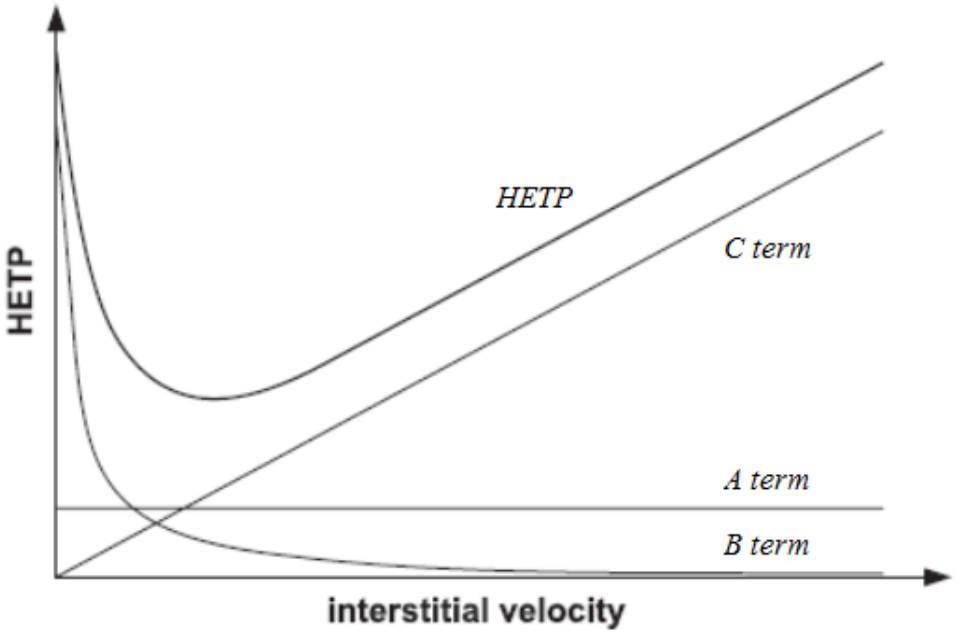

Figure 1.1. Dependency of HETP from mobile phase velocity (Schmidt-Traub 2005, 54).

The van Deemter equation has three terms, which characterize various effects that need to be considered in preparative chromatography during choosing stationary phase. The first term A is eddy-diffusion parameter and can be calculated by Eq. 1.7. This parameter is almost constant throughout the range of velocity. It occurs from both wide distribution of particle size of the adsorbents and unideal packing. As this term is proportional to d_p, it could be decreased by using smaller particles and thus the HETP will be lower, too. However, the average particle diameters, which are applied in industry, are in range 0.2-0.4 mm. The utilizing of larger diameter particles associated with finding a balance between separation efficiency, expressed in the form of mass transport, and costs (investment and operating), in the form of pressure drop (Sainio et al. 2011, 146).

$$A = \frac{d_p}{L} \tag{1.7}$$

where d_p is particle diameter.

The second term B is expressed by the hyperbolic curve and it is molecular diffusion parameter. However, influence of B can be seen only during operating with low mobile flow velocities with large diameter particles in preparative chromatographic equipment. The As the rate of flow rate is usually high in preparative scale, the term B can be neglected. Changing the mobile phase composition by using solvents with low viscosity

leads to obtaining lower pressure drops of column and high diffusion coefficients. The B parameter can be found by:

$$B = 2\frac{D_m}{L} \tag{1.8}$$

where D_m is molecular diffusion.

The third term C corresponds to the increase of the HETP at high rates at linear dependence. It is occurred because of the growth of impact of mass transfer resistance (MTR) at higher rates. In general case, MTR is independent of flow rate, especially inside the pores, but with increasing the rate of mobile phase the relation dominates between MT into and in the adsorbent and the convective axial transport in the column mobile phase. The nature of adsorbent affects on the slope of the parameter C. If packing material has optimized diffusion pathlength and accessibility of pores, then the slope of the C would be lower and, thus, column would have the higher NTP at high flow rates. The determination of the parameter C is presented in the form of Eq. 1.9.

$$C = 2\frac{K'}{(1+K')^2}\frac{t_m}{L} \tag{1.9}$$

where K' is retention factor and t_m is global mass transfer time.

All the columns don't have same number of theoretical plates. Generally in preparative scale it ranges lower than 1 000, but it also depends on the mobile phase velocity, its viscosity and molecular of compound to be separated (Rathore 2003, 30-40).

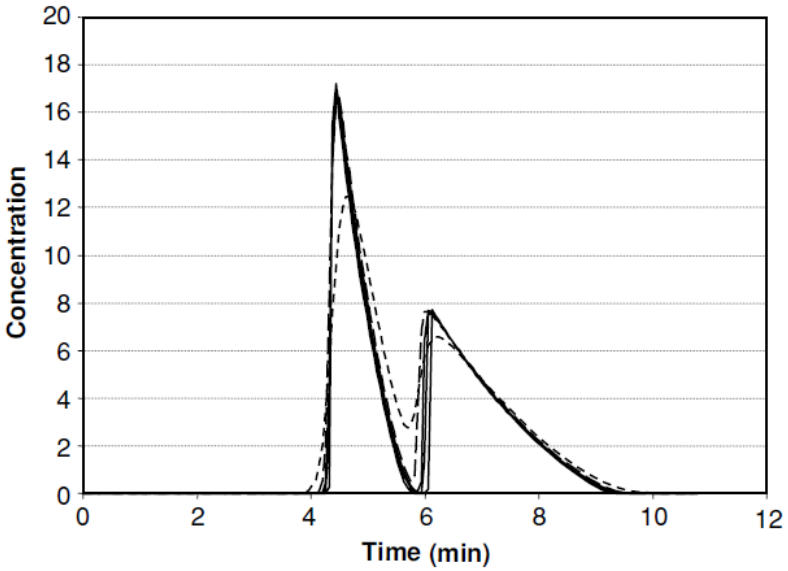

Figure 1.2. Band profiles of preparative separation process with different NTP. Short dashed line corresponds to 200 plates, long dashed – 500 plates and other lines 750-2000 plates (Cox (ed.) 2005, 34).

In Fig. 1.2, it is shown that with increasing number of theoretical plates concentration of the component becomes higher and concentration profile - narrower.

1.1.3 Performance parameters of preparative chromatography

The most important performance parameters are recovery yield, purity, eluent consumption and productivity.

From the ratio between the amount of the product component and the sum of all amounts in that fraction the purity could be defined (Siitonen and Sainio 2014, 18).

$$P_i^j = \frac{m_i^j}{m_1^j + m_2^j} \cdot 100,\ \% \tag{1.10}$$

where m_i^j is a quantity of the component i in the product stream j.

The ratio between the amount of the product collected and injected amount of the component in fresh feed stream defines the recovery yield.

$$Y_i = \frac{m_i^j}{m_i^F} \cdot 100,\ \% \tag{1.11}$$

where upper index F means the fresh feed stream.

The eluent consumption, as the parameter with the main part of the operational cost, can be derived by the ratio between the total amount of eluent required in separation cycle and the sum of the amount of products.

$$EC = \frac{V_{eluent}}{m_1^A + m_2^B} \tag{1.12}$$

where V_{eluent} is the amount of solvent used in cycle.

The final performance parameter is productivity, which is derived by the ratio between the sum of amount of components in desired product streams and cycle time in column with the certain volume (Gottschalk (ed.) 2009, 225).

$$PR = \frac{m_1^A + m_2^B}{V_{column}\Delta t_{cycle}} \tag{1.13}$$

where V_{column} is total volume of considered column and Δt_{cycle} - cycle time.

The productivity is a scalable parameter, which can be applied for a large scale predicting of the requirements for chromatographic separation (e.g., equipment, materials) from using PR measurements obtained by small column. This parameter has dimensions as mass of product per mass of adsorbent per day (kg/kg/day or kkd). The chromatography process could be divided into the following meanings: poor (when PR is equal to 0.1 kkd or lower), optimal (PR near 1 kkd) and really great (with PR values greater than 10 kkd). The estimating of the productivity can be done by loading studies (Cox (ed.) 2005, 7-8).

As it could be seen from Fig. 1.3, which is a one example, with given *PR* of the separation the column length (x-axis) and production rate (y-axis) can be found.

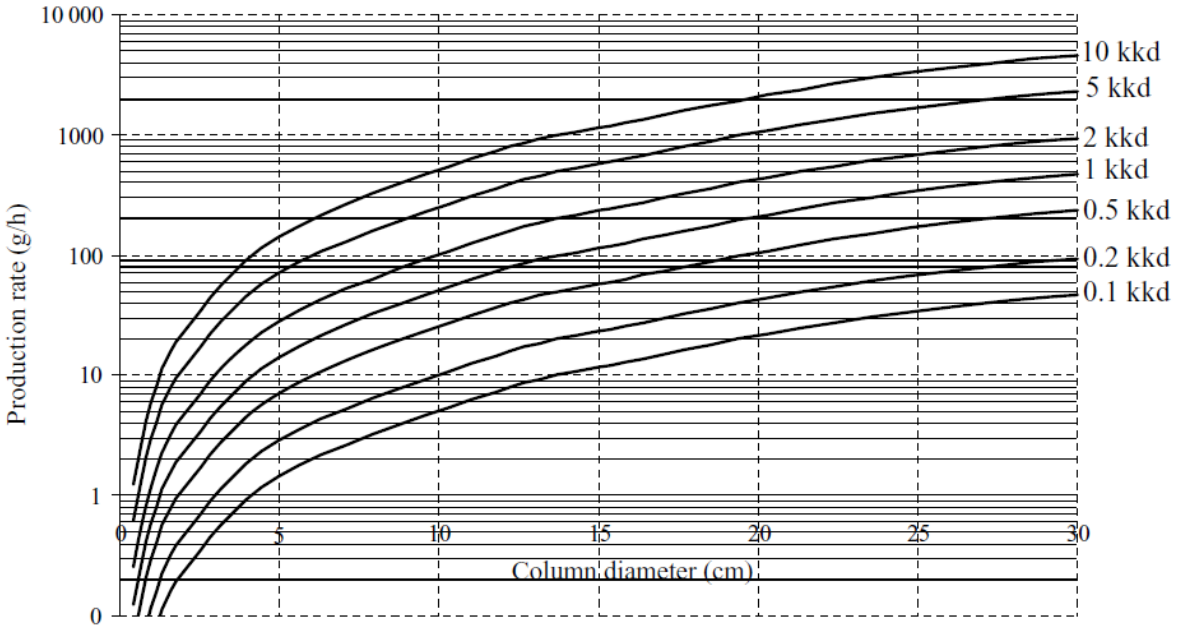

Figure 1.3. The dependence of the production rate from the productivity and diameter of column (Cox (ed.) 2005, 7).

In case of the impact of different adsorption and column parameters on the productivity, there is the research (Forssen et al. 2014, 1-8), where it was investigated that the increasing of *PR* achieved by the following: the use of short columns, rising the pressure drop over it, reducing the viscosity of the mobile phase and the use adsorbent particles as smaller as it possible. There are also some limitations for these ways, which are detailed considered in the same research (Forssen et al. 2014, 1-8). In additional to them, the separation factor α should be larger than 2 (this is crucial parameter for the last product component than the first), but no significant increasing because of small changing of the maximum *PR*; it was also found that increasing the saturation capacity of the adsorbent and reducing the retention factor of the first compound product cause rising of *PR* and the extension of

number the theoretical plates and feed concentration do not affect significant on the maximum *PR*.

1.2 Equilibrium Isotherms

With certain constant pressure and temperature the equilibrium isotherm can be plotted. It is a plot, where abscissa variable is the equilibrium concentration of solute in the stationary phase and ordinate variable – the equilibrium concentration of solute in the mobile phase. The solute molecular cooperation with these phases affect the thermodynamic properties which are mentioned above. The equilibrium isotherms define the band profiles with high concentrated solute (Guiochon et al. 2006, 68-69). In chromatography separation performance cannot be poor, therefore any deviation from equilibrium state is undesirable and also leads to the variation for mass transfer kinetics.

The higher of the feed load increases the component concentration into the mobile phase, consequently, increases it in the stationary phase as well. Due to the fact that the chromatographic column has a certain amount of adsorbent, it is possible to overload it with high enough feed load and what kind of effect will be is determined by the adsorption isotherm shape and curvature. With low concentrations of the feed the isotherm is usually linear, in case of high concentration the isotherm is defined by a complex function of the cooperation between the solute molecules and reacting sites of adsorbent, interaction of molecules which are adsorbed with those which are in mobile phase.

The Linear Isotherm

The linear isotherm, as the simplest isotherm, in final equation can be expressed by:

$$q = HC = k' \frac{\varepsilon}{1-\varepsilon} C = \frac{k'}{F} C \tag{1.14}$$

where H is the Henry's constant (usually it is the dimensionless parameter), k' - the retention factor (which is equal to $k' = \frac{(t_R - t_0)}{t_0}$, where t_0 is dead time), $F = \frac{V_s}{V_m} \frac{(1-\varepsilon)}{\varepsilon}$ is the phase ratio, which is equal to the ratio between the volume of the adsorbent V_s and the volume of mobile phase V_m, and ε is total porosity of the considered column.

From the Eq. (1.14) it is clearly seen that the solute concentration in mobile phase is directly proportional to that in the solid phase. In this equation the Henry's constant is

responsible for the slope of the isotherm. With higher concentration the isotherm becomes nonlinear because competitive interactions occur between different solute molecules and adsorption sites. Thus, after getting experimental results, more complex function is needed for their characterization (Guiochon et al. 2006, 73). The linear isotherm is given on Fig. 1.4.

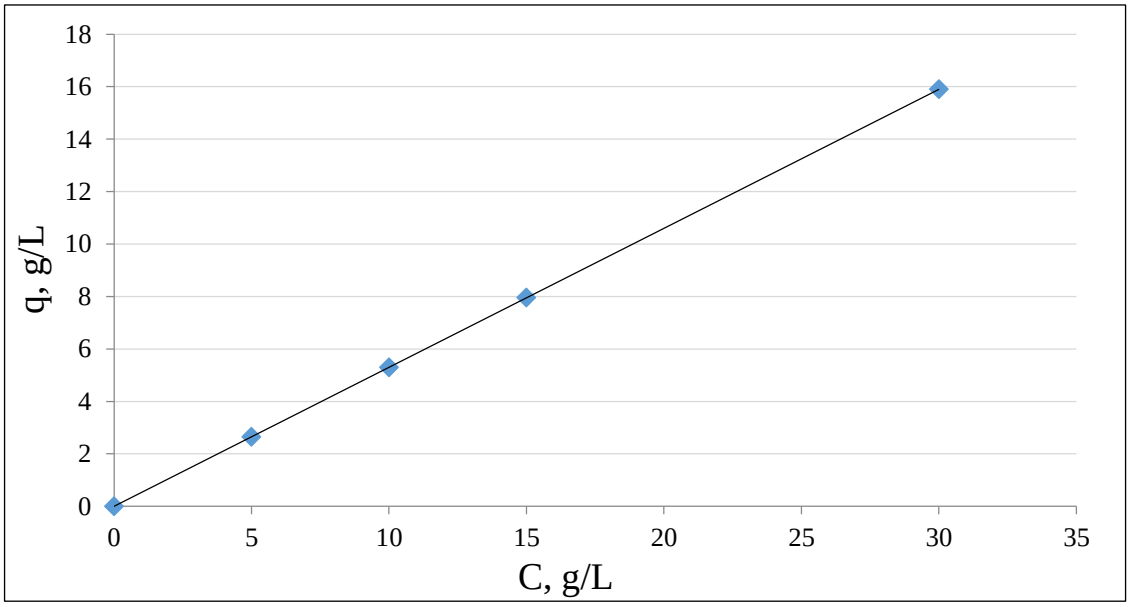

Figure 1.4. The example of the linear isotherm for fitting the experimental data of fructose. Parameter H = 0.53 (Coelho et al. 2002, 2-3).

The Langmuir Isotherm

In preparative chromatography the most frequent type of isotherm is the Langmuir isotherm. This type is used when the adsorbent surface is homogeneous and higher concentration is presented and competitive interactions occur between different solute molecules and finite number of adsorption sites. It was established that the Langmuir isotherm is suitable for a wide range of concentrations and has a good approximation for fitting obtained experimental data (Guiochon et al. 2006, 81-87). This isotherm is defined by the Eq. (1.15) and presented in Fig. 1.5.

$$q = \frac{Ca}{1+Cb} = \frac{q_s Cb}{1+Cb} \tag{1.15}$$

where a and b are numerical coefficients; q_s is adsorbent saturation capacity (solid phase), which is determined by the ratio between numerical coefficients (a/b). In case of high solute concentration the term signifies the limit of the stationary phase. This parameter can be referred either to specific or column saturation capacity.

The fractional surface coverage is expressed by the ratio $\theta = q / q_s$ and, thus, the equation of isotherm becomes as following:

$$\theta = \frac{bC}{1+bC} \tag{1.16}$$

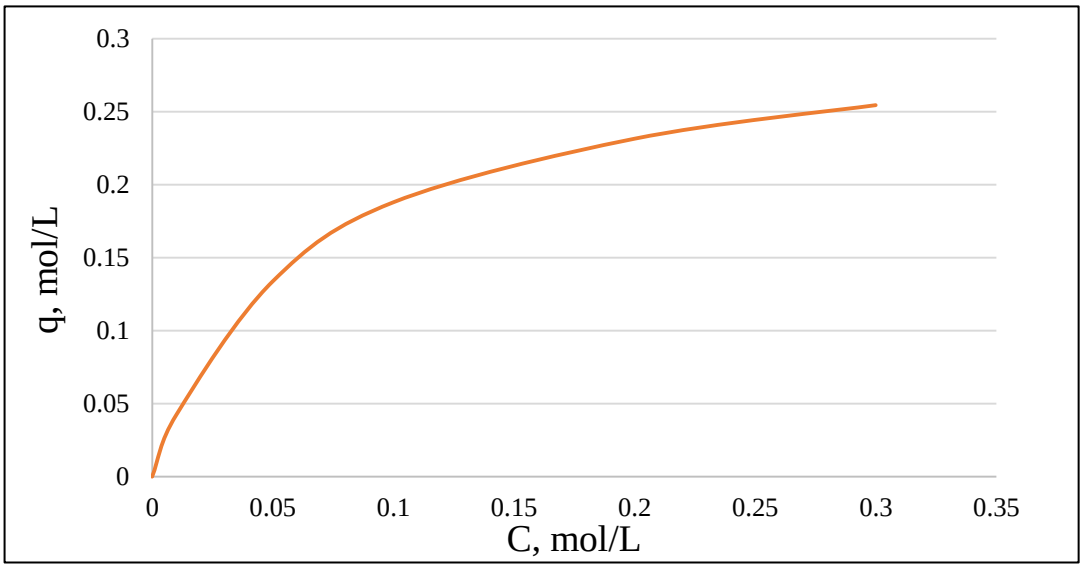

Figure 1.5. The example of the Langmuir isotherm. Parameters: q_s = 0.319, b = 14.2.

Other types of isotherms

The above mentioned isotherm assumes homogeneous adsorbent surface, but it may not be so. With complex surfaces occur new parameters and the curve description becomes complicated. There are various isotherm equations which have been suggested and where new variables were taken into account, for example: the Freundlich isotherm describes the equilibrium in low solute concentration with assuming infinite retention of everything; the Bi-Langmuir isotherm describes a nonhomogeneous surface with patches made of different homogeneous surfaces; 'S-shaped' isotherms includes the solute molecules stacking and others (Guiochon et al. 2006, 89-107).

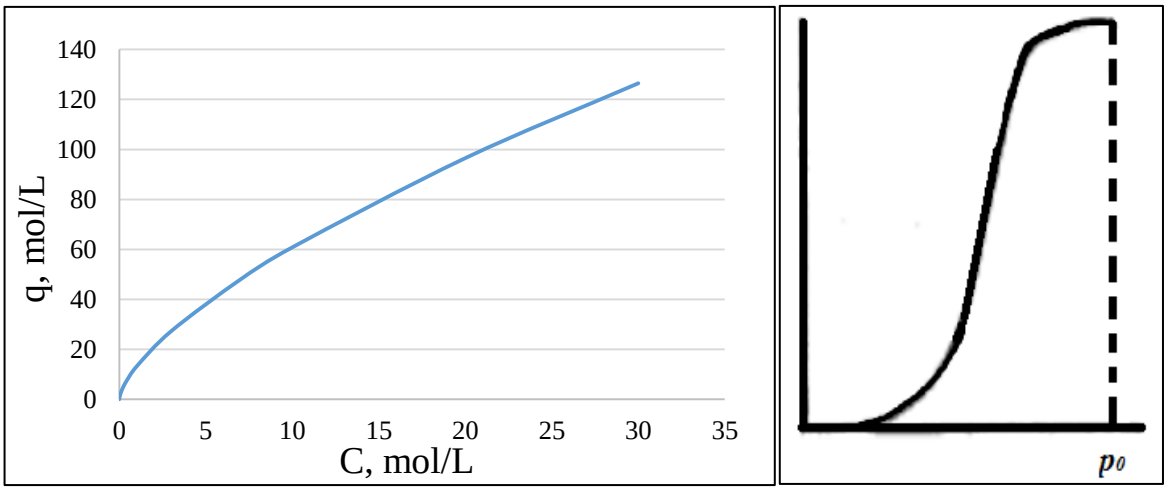

Figure 1.6. The example of the Freundlich (left) with parameters n=1.5, a =13.1 and illustration of 'S-shaped' (right) isotherms.

1.3 Transport occurrence in chromatography

The collecting of the product components with the highest concentration is the main purpose of the chromatographic separation in preparative and industrial scale. When the solute components injected into the column, achieving a rectangular signal of separation with concentration and time interval as initially is possible only in ideal conditions. In reality deviation from the rectangular band profile takes place. There are factors which impact on the shape and broadening of chromatographic peaks: mass transfer resistance and non-idealities in fluid distribution (the term axial dispersion is used and it includes all hydrodynamic effect).

1.3.1 Differential mass balance in chromatographic column

For determination of band profiles of chromatographic separation the differential mass balance is required. In this case, there are two assumptions that the column is considered uniform (or in other words radially homogeneous) and it has constant properties (Guiochon et al. 2006, 21-23). The differential mass balance equation for the compound i can be expressed by:

$$\varepsilon S\left(uC_i - D_{L,i}\frac{\partial C_i}{\partial z}\right)\Big|_{z,t} - \varepsilon S\left(uC_i - D_{L,i}\frac{\partial C_i}{\partial z}\right)\Big|_{z+\Delta z,t} = \Delta z S\left(\varepsilon\frac{\partial C_i}{\partial t} + (1-\varepsilon)\frac{\partial C_{s,i}}{\partial t}\right)\Big|_{\bar{z},t} \qquad (1.17)$$

where $C_{s,i}$ and C_i are the stationary and mobile phase concentrations of the component, which are functions of time t and length variables $z, \Delta z$ (distance along the column and

the thickness of the slice of column); $D_{L,i}$ is axial dispersion coefficient; u is the mobile phase velocity and $S = \pi d_c^2 / 4$ is the column cross-sectional area.

Provided that $D_{L,i}$ and u are constant lengthways the column, it gives a second order partial differential equation:

$$\frac{\partial C_i}{\partial t} + F\frac{\partial C_{s,i}}{\partial t} + u\frac{\partial C_i}{\partial z} = D_{L,i}\frac{\partial^2 C_i}{\partial z^2} \tag{1.18}$$

In Eq. 1.18 the right-hand side term corresponds to the diffusion term and on the LHS two accumulative terms relevant to the changing of the component concentration in mobile and solid phase by time and third is convective term, respectively. For each component the second order partial differential equation must be written.

1.3.2 Fluid distribution in packed bed

In column chromatography the distribution of fluid plays significant role in term of the axial dispersion and, thus, in band broadening. There are four effects of the fluid distribution that cause non-idealities: microscopic, mesoscopic and macroscopic (Schmidt-Traub 2005, 20-23).

The first effect is associated with the fluid dynamic adhesion, which occurs inside the microscopic channels at the solid phase between the solution and the pellets of adsorbent. Due to adhesion, the rate of the mobile phase in the middle of channel is higher and retention time of the solute molecules becomes lower than near it walls. It is clearly represented by the Fig. 1.7a. The voidage non-uniformities and the formation of impermeable agglomerates by adsorbent particles are another reason for the band broadening by axial dispersion.

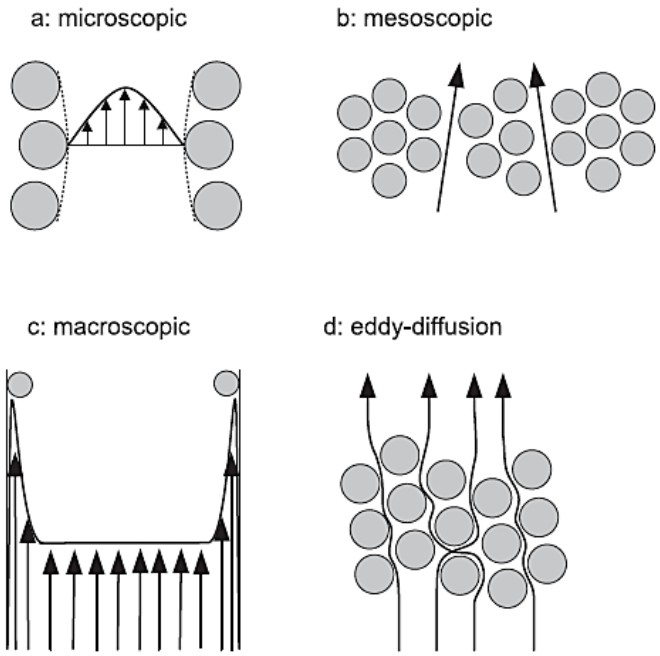

Figure 1.7. Schematic representation of non-idealities of fluid distribution (Schmidt-Traub 2005, 23).

The second effect leads to differences in the rate of mobile phase (Fig. 1.7b) and various length of the solute molecule way passing through and around the pellet aggregates (Fig. 1.7d). The latter effect is called eddy-diffusion and it is a part of the mesoscopic effect because of overall similarity.

The last one is macroscopic effect which is shown on Fig. 1.7c. This effect is related with irregularity of the packing and, thus, different voidage, which are most common near wall region.

1.3.3 Mass transfer

In preparative chromatographic separation porous particles are used more often than non-porous because of their well-defined pore structures and significantly larger surface for adsorption than non-porous. The efficiency of chromatography depends on adsorption of the solute molecules inside the pore of a pellet. Besides axial dispersion, the mass transfer factors, which are presented on the Fig. 1.8, also affect the band broadening (Schmidt-Traub 2005, 23-25).

Every single adsorbent particle of the stationary phase is coated by the stagnant film of the mobile phase, which has some thickness depending on the fluid distribution in the channels at the solid phase between the solution and the pellets of adsorbent. The first step of the

mass transfer of the solute molecule is the movement to the boundary layer (1). This transporting occurs by diffusion or convection.

The next step (2) of the molecule path is film diffusion. It is the molecular transfer through the boundary layer. After this step the diffusion of the solute molecule accompanied by two transport mechanisms, which are pore and surface diffusion.
In the case of surface diffusion the adsorptive species are adsorbed and moved further to the center (in the depth) of particle along the pore surface under the influence of the attraction forces (3b). Due to the fact that the attraction forces are very strong, in the industrial scale systems surface diffusion is considered as instantaneous step and the solute molecule can't move deeper attached place.

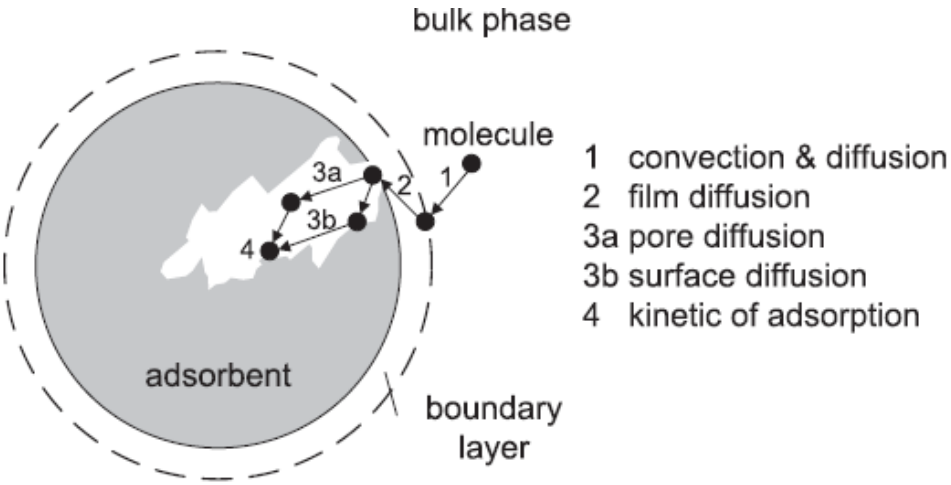

Figure 1.8. Mass transfer occurrence (Schmidt-Traub 2005, 24).

During the pore diffusion the attraction forces of the surface of solid phase do not act and this transfer process goes by Fickian diffusion of the adsorptive species (3a).

The final step (4) is kinetics of adsorption and desorption. It occurs when a molecule occupies a free adsorption place inside the pore of particle.

If the convective mobile flow would be faster than the mass transfer processes 1-4, then chromatographic peaks will have a nonsymmetrical behavior of band broadening. In additional, serious tailing might appear when the solute molecules move further in the depth of the pore and, thus, their movement becomes slower.

The first and forth step in the mobile phase are usually very fast. The second and third steps are speed limiting processes. In the case of industrial scale chromatographic

separation, when diameter of particles is larger than $5\,\mu m$, the pore and surface diffusion play crucial role in term of MTR. To characterize mass transfer resistance, there is effective mass transfer coefficient, k_{eff}, which is applied as model parameter. For example, typical k_{eff} for glucose is equal to the range $7 \cdot 10^{-4}$ cm/s to $5.7 \cdot 10^{-5}$ cm/s and for fructose from $6.5 \cdot 10^{-5}$ cm/s to $8.9 \cdot 10^{-5}$ cm/s (Schmidt-Traub 2005, 448).

As the resistance of mass transfer depends on the two main mechanisms, their speed is affected by the surface chemistry and the nature (structure) of the adsorbent particles. The pore size affect in two different ways. Firstly, the total pore size. The pore can accommodate more solute molecules than available adsorption sites are and, thus, some of them cannot be adsorbed. Moreover, for molecules with bigger size the limitation of the accessible surface area takes place. Secondly, all adsorption sites should have equal both the diffusion pathway and unhampered general availability. Due to the fact that the movement of the solute molecules is diffusive within a mesoporous system, the size distribution of the adsorbent particles plays significant role in increasing the band broadening. It happens because with larger pores molecules adsorb faster and therefore the residence time of molecules in mobile phase is shorter than it is in the smaller pores.

The main physical property of the adsorbent is available surface area. In the ideal case, it is so high, that provide numerous of adsorption sites, which have short diffusion pathways. Moreover, all pores of the adsorbent should be of same size with acceptable depth and with equal availability of the pore from the convective flow area.

In order to determine pore diameter, $d_{pore}\,(nm)$, which is assumed to be constant, there are following parameters: specific surface area $S_{BET}\,(m^2/g)$ and volume of the pore $V_{pore}\,(ml/g)$. These parameters are interconnected and, consequently, their relationship can be defined by Wheeler equation:

$$d_{pore} = 4 \cdot 10^3 \left(\frac{V_{pore}}{S_{BET}} \right) \tag{1.19}$$

During the adsorbent engineering for preparative chromatography, there is a choice to create fragile particles with high surface area and with enough amount of adsorption sites or to create durable pellets with small surface area.

1.3.4 Diffusion

The adsorbents used in preparative scale comprise of particles which are formed by small micro- or non-porous crystals. As it was mentioned in previous section, the solutes from the bulk phase transfer to the particle surface and then through the boundary layer. After that the adsorptive species diffuse within the pellet pores. The surface and pore diffusion usually are the speed limiting processes and, thus, their contribution to the MTR is rather high.

Pore diffusion

The adsorption of the solutes accompanied by the following processes: transporting occurs by diffusion or convection to the boundary layer, penetration through the film, pore and surface diffusion inside pore, adsorption and desorption and finally diffusion out of the pellet. Pore diffusion can occur by the 4 mechanisms which are typically combined: surface diffusion, Poiseuille flow, molecular diffusion and Khudsen diffusion (Guiochon et al. 2006, 250-257). Their speed depends on the parameters of the pore (i.e. the pore tortuosity, size, narrowing and network connectivity), the concentration of the solute molecules, etc. During the experimentally measurement of the effective pore diffusivity is taken into account the effect of multiple mechanisms.

It is hard to predict the effective pore diffusion because of large number of factors that should be considered, particularly the pore structure. This diffusion occurs inside the pore volume and also in the bulk phase, where near the surface of particles the electromagnetic field is.

The pore diffusivity could be defined with using cross-section area of the pore:

$$J = -\varepsilon_p D_p \frac{dC}{dz} \tag{1.20}$$

where D_p is the pore diffusivity and ε_p - is intraparticle porosity.

Because of the difference in shape and structure of the pore, the pore diffusion coefficient is smaller than the diffusivity in “ideal” cylindrical pore, D. This difference is characterized by the various trajectory of the pores with following growth of the distance of the diffusion pathway and the non-permanent pore diameter. Therefore, for considering

the above two effects the tortuosity factor is suggested and the pore diffusivity equation is presented as:

$$D_p = \frac{D}{\tau} \tag{1.21}$$

where τ tortuosity factor, the value of which is 3-5 (Sheng 1995, 141-142 and Camacho-Rubio et al. 1995, 937-938).

Surface Diffusion

During the movement of the solute molecules along the macropore surface the surface diffusion takes place.

In most cases it was assumed that molecules, which are adsorbed, become attached to the adsorption site and cannot move further. However, sometimes this immobile state does not occur. There are reasons, which are related with surface energy and with the nature of the solute molecules, when adsorbate species can stay motionless or can transfer under the electric field along the stationary phase surface. Surface diffusion is also possible when the adsorbate species do not need to be desorbed (they are moving near the surface), because under specific conditions the energy of desorption may be higher than the activation energy of their motion.

When the surface diffusion occurs, the effective diffusion coefficient D_e is derived from the sum of both pore D_p and surface diffusion D_s and can be written as:

$$D_e = D_p + \rho_k H D_s \tag{1.22}$$

where ρ_k is the density of adsorbent particle and H is the Henry constant when linear conditions are.

As for example, the value of diffusion coefficient in aqueous solutions for fructose is ranged from (0.69 to 0.94)$\cdot 10^{-8}$ m^2/s and for glucose it is from (0.68 to 0.97) $\cdot 10^{-8}$ m^2/s depending on temperature, 25°C and 39°C, respectively (Ribeiro et al. 2006, 1838).

1.3.5 Axial dispersion

In order to define axial dispersion, the band profile of penetrating tracer is used. It also can be determined by Eq. 1.23 where the first part of the sum is molecular diffusion contributor and the second is eddy diffusion (Guiochon et al. 2006, 244-246).

$$D_L = \gamma_1 D_m + \gamma_2 d_p u \tag{1.23}$$

where γ_1 is the (external) tortuosity, D_m is molecular diffusion coefficient, γ_2 is the packing factor (should be determined for different velocities) and d_p is the diameter of the particle.

The contribution of D_m is insignificant and, therefore, the axial dispersion becomes approximately a linear dependent of the velocity:

$$D_L = \gamma_2 d_p u \tag{1.24}$$

The values of axial dispersion coefficient vary in the order of 10^{-4} cm^2/s (Guiochon et al. 2006, 506). In particular case, the dependence between D_L (cm^2/min), and interstitial fluid velocity, u_L (cm/min), was obtained for glucose, $D_L = 0.057\,u^{:L}$, and for fructose, $D_L = 0.077\,u^{:L}$ (Lee 1996, 67-73).

For wide range of Reynolds number axial dispersion could be defined from the Peclet number by the equation of Chung and Wen in packed beds:

$$Pe = \frac{L}{\varepsilon\, d_p}\left[0.2 + 0.011\mathrm{Re}^{0.48}\right] \tag{1.25}$$

where ε is external porosity.

After substitution $Pe = \frac{uL}{D_L}$, axial dispersion is equal to (Schmidt-Traub, 2005, 51-54):

$$D_L = \frac{u d_p \varepsilon}{0.2 + 0.011(\varepsilon\,\mathrm{Re})^{0.48}} \tag{1.26}$$

1.3.6 Pressure drop

During the fluid flow, its velocity is different in space. With the direct flow in tube fluid has the friction near walls and that is why velocity is lower than at the center of flow. Thus, the layers at different distances from the wall are moving with various velocities slide relative to each other, overcoming internal friction which depends on the viscosity coefficient. In order to overcome this internal friction it is necessary to apply an external force – pressure drop between the ends of tube. With increasing length of column, area of

sliding layers and therefore the friction force are increasing and for that it is required bigger pressure drop (Sakodynskiy et al. 1993, 22-28).

The eluent viscosity depends on the total viscosity of the mobile phase and the fresh feed with solute molecules, if they are vary. Therefore, the pressure or flow rate becomes dependent on the eluent viscosity. When assuming the constant rate of flow, the pressure will be varied and, consequently, with high viscosity flows operating pressure will be increased. And the concentration profile of adsorptive species in the eluent (with constant flow rate) could be found as a time function (Guiochon et al. 2006, 267-269). Then viscosity profile is determined and with local value of the viscosity $\eta_{m,i}$ at the slice of column with length, Δz, the local pressure drop (with the value of the local viscosity) is calculated with following equation:

$$\Delta P = \frac{u\Delta z}{k_0 d_p^2}\eta_{m,i} \tag{1.27}$$

The local pressure drop can be integrated along the length of column L, expressed by $N = \frac{L}{\Delta z}$, and then the overall pressure drop defined as:

$$\Delta P = \frac{u\Delta z}{k_0 d_p^2}\sum_{i=1}^{N}\eta_{m,i} \tag{1.28}$$

Typically, with particles as a stationary phase, the Ergun equation (Eq. 1.29) is used for pressure drop calculation.

$$\frac{\Delta p}{L} = \frac{150\eta(1-\varepsilon)^2 u_0}{\varepsilon^3 d_p^2} + \frac{1.75(1-\varepsilon)\rho u_0^2}{\varepsilon^3 d_p} \tag{1.29}$$

where u_0 is the superficial velocity of fluid and η is the fluid viscosity.

After substitution by packing coefficient $k_0 = \frac{\varepsilon^3}{150(1-\varepsilon)^2}$, which has the range 0.5-2$\cdot 10^{-3}$, the Eq. 1.29 could be transformed to Darcy's law equation and pressure drop is defined by:

$$\Delta P = \frac{1}{k_0}\frac{\eta u_0 L_c}{d_p^2} \tag{1.30}$$

The Eq. 1.29 shows the dependence of the pressure drop from the porosity. The void fraction with the particles, which have different diameter, can reduce enormously. It is more important when operating of analytical chromatography and the distribution of particle size should be near 2. For the industrial scale separation with larger diameter of particles, the particle size distribution can be accepted with higher values (Schmidt-Traub 2005, 56-57).

1.4 Ion Exchange

The chromatographic separation is often applied in the sweetener industry. The major adsorbents, which are used in the chromatographic columns, are ion exchange resins (Sainio et al. 2011, 146). The properties of the resins affect the performance of the whole process.

The framework (matrix) of ion exchanger has a "+" or "-" electric excess charge. This surplus is balanced by counter ions of opposite sign which can be replaced during exchange process by other ions of the identical sign (Fig. 1.9). Cation exchangers contain cations, and anion exchangers anions, as counter ions. The process of exchange is usually reversible and stoichiometric. Generally, the ion exchanger has the property of selectivity, i.e., it takes up a certain counter ions in preference to others. (Helfferich 1995, 14-17).

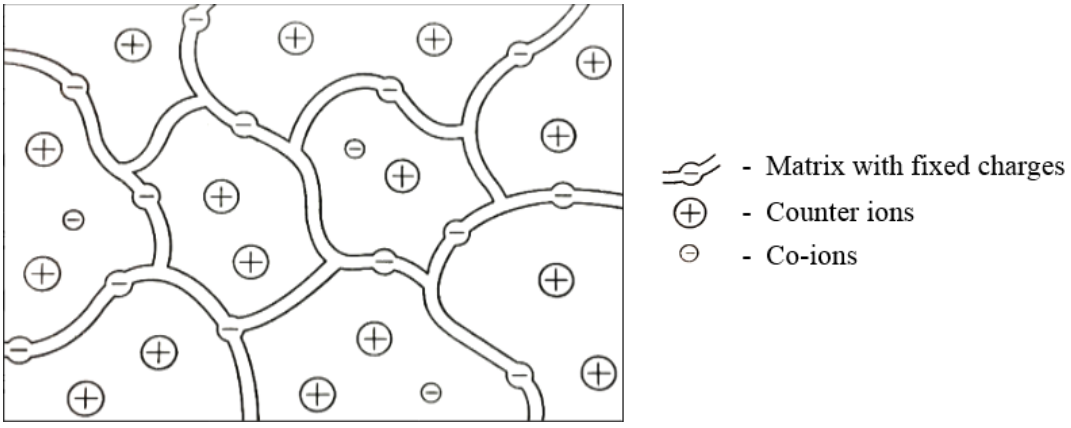

Figure 1.9. Schematic structure of an ion-exchange resin (Helfferich 1995, 15).

The organic ion-exchange resins have gel-type macrostructure and their framework comprises a 3D hydrocarbons chains network which is irregular and macromolecular. The physical properties of the resins (e.g., mechanical, chemical and thermal resistance) and the behavior of ion-exchange process depend on the degree of framework crosslinking and matrix structure and on the number and nature of the ionic fixed groups.

The degree of matrix crosslinking characterize the following parameters: the counter ions mobility in the resin and the swelling ability of resin, which is depend on the framework mesh width. Generally, the crosslink density of the ion-exchange resins, which are utilized in industrial scale chromatography, is varied from 5 to 8 wt-% (Sainio et al. 2011, 146). The counter ions mobility characterize the rates of ion-exchange and other processes and the electric conductivity of the resin.

There are four main types of functionality of resins: strong acid or weak cation, strong base or weak anion. Their operating capacity is pH-dependent.

1.4.1 Cation Exchange Resins

The first type of cation exchange resins is strong acid cation or SAC which have a styrene or acrylic skeleton. The most typical representative is sulphonated polystyrene-divinylbenzene (or PS-DVB) resin, and could be cross-linked with alkenylaromatic polymer resins (e.g., monomers of alkyl-substituted styrene) or other aromatic or aliphatic crosslinking monomers, for example, divinyltoluene, divinylxylene or ethylene glycol dimethacrylate, N,N'-methylene bisacrylamide, respectively (Liberti and Helfferich (ed.) 1983, 23-30). These strong acid cation resins are in prevalence compared to other types due to their durability and low cost.

The second type is weak acid cation (or WAC) exchange resins which have mostly acrylic or methacrylic skeleton with carboxylic functional groups. Also it could be, for example, a styrene resin with another weak acid as the functional group. Methyl acrylate, ethyl acrylate, butyl acrylate, acrylonitrile or acrylic acids or their mixtures provide the basis for the producing an acrylic resin. The resin may be cross-linked with a cross-linking agent that are mentioned above (Saari 2011, 16).

1.4.2 Anion Exchange Resins

As SAC exchange resins, strong base anion (SBA) exchange resins have a styrene or acrylic skeleton. The cross-linking agent may be DVB or other alkenylaromatic polymer, e.g., alkyl-substituted styrene or their mixtures or with other already mentioned suitable aromatic cross-linking monomers.

Weak base anion (WBA) exchange resins have methacrylate-DVB exchanger with dimethylamino-propylamine as the functional group. This type of resin is the newest and, thus, have lacking applications in preparative scale (Saari 2011, 17).

1.4.3 Selective separation of individual monosaccharides

The chromatographic separation is widely used in the sugar industry to separate individual sugars from sugar syrups obtained from sugar cane or sugar beet. The enrichment of fructose in fructose-glucose syrups is the most prevalent separation process in sweetener industry which is based on SMB chromatography. This syrup is derived from hydrolysis of sucrose to fructose and glucose. In the sugar industry the most suitable and widely used adsorbent is sulfonated SAC PS–DVB resin in Ca^{2+} form because of their higher capacity, selectivity and chemical inertness.

The mechanism of the chromatographic separation of individual monosaccharides from their mixture is mainly ligand exchange. The formation of complexes between monosaccharides and the metal counter-ions of the resin causes the fractionation of monosaccharides. The mechanism that occurs in separation of larger sugars (e.g., sucrose, oligosaccharides) is predominantly size exclusion: totally or partially exclusion of larger molecules from the resin and weakly interacting only with the metal counter-ions of the resin (Heinonen and Sainio 2013, 340-341).

For chromatographic fractionation of sugars the metals from groups I and II are used, e.g., the most commonly is Ca^{2+} and also Na^{+}, K^{+}, Pb^{2+} as the counter-ions can be applied. In addition, there are also another adsorbents, e.g. aluminas and zeolites, which have been investigated for sugar separation (Masuda et al. 2002, 89-96). But only SAC exchange resins have wide application in industry because of their high selectivity for fructose (Luz et al. 2008, 2455-2465). The complexes between monosaccharides and the metal counter-ions, which are formed during separation, vary in strength because of different molecular structures of the monosaccharides.

There are different researches where comparison between various ions as counter-ions in resins was made. At first one it was between for gel-type resin in K^{+} and macroporous resin in Na^{+} form (Nobre et al. 2009, 71-76). It was found that at the operational temperature 25 $^{\circ}$C the best choice is the K^{+} form resin, which shows higher selectivity and better separating of mixtures of fructose and glucose. Another research was made with Ca^{2+}, K^{+} and H^{+} ions as counter-ions in case of separation of lactobionic acid, lactose, sorbitol and fructose (Pedruzzi 2008, 600-611). It was investigated that for this quaternary separation K^{+} form resin was to be more suitable, but another fact was also confirmed that

Ca^{2+} ions have a higher separation factor for fructose/lactose and sorbitol/lactose due to formation of complexes.

Typically, the aqueous eluent is used in chromatographic separation processes of monosaccharides with neutral or acid pH. There is a special research for using eluent in subcritical water form at moderate pressures and extend this applying to the preparative scale (Tiihonen et al. 2005, 166-174). The adsorbent and components thermal stability (e.g., carbohydrates) are the limiting factor for using this type of eluent. The result of the performed experiments is the confirmation that operating of separation process with the temperature over normal boiling point of water increases the efficiency of separation of carbohydrates. This growth is reflected by the decreased separation time and, in some cases, resolution increasing. Additionally, the using of higher solutes concentration then can be applied. Moreover, it was shown that the temperature stability of the carbohydrates, during increasing of operating temperature, is the predominant limiting factor. For the sugar alcohols there was not any degradation at the temperatures up to 448K. However, the maximum temperature during the chromatography process without degradation of sugars was determined at the 398K and, therefore, it should be below this value.

Adsorption isotherms in sugar separation with ion exchange resins

For predicting band profile of chromatographic separation of components, it is needed to know the equilibrium isotherms (Kuhn et al. 2012, 127-133). The separation and purification of carbohydrates is a broad field encompassing molecules having substantially different physical properties. Monosaccharides (or simple sugars), as the basic unit of carbohydrates, are comprised of a single saccharide unit and that is why hydrolyzation to simple compounds cannot be done (Linhardt and Bazin 2001, 53-55). Their formula is $C_nH_{2n}O_n$.

The enrichment of fructose in fructose-glucose syrups is the most prevalent separation process in sweetener industry which is based on SMB chromatography. The separation of both isomers (glucose and fructose) performs with high efficiency by cation exchange. Due to the fact that the adsorption behavior of sugars is linear during a broad range of concentrations and the importance of producing of high-fructose corn syrup in industry is, there are a lot of scientific researches related with glucose fructose separation (Xie et al. 2001, 363-375).

The single component isotherms for sugars were obtained in one research by using static method (Gramblicˇka and Polakovicˇ 2007, 345-350) and they were plotted for different types of resins (see Fig. 1.10). From the figure below, it is seen that for glucose the behavior of concentrations in stationary and mobile phases is expressed by linear dependence.

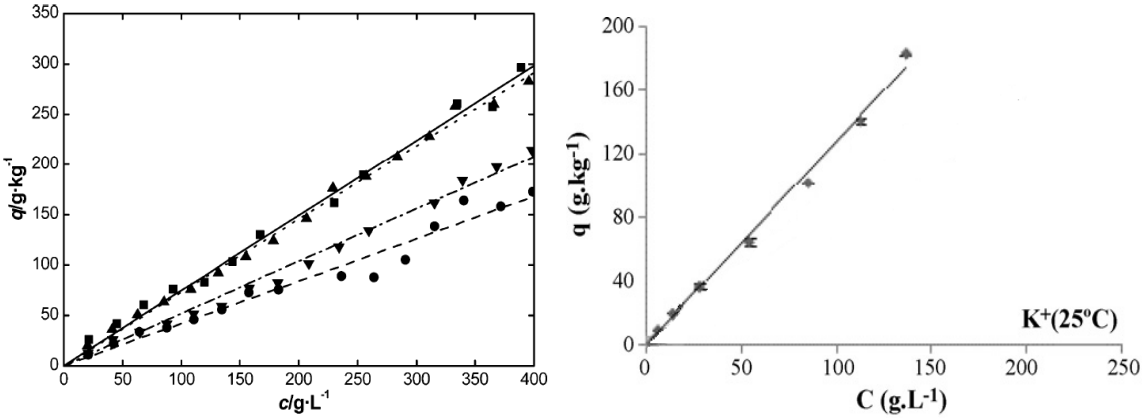

Figure 1.10. The glucose (left) and fructose (right) adsorption isotherms. Left: the upper isotherms are for K^+ form resin (Gramblicˇka and Polakovicˇ 2007, 349) and below them - for Ca^{2+} form resin; right: for K^+ form resin (Nobre et al. 2009, 3).

Furthermore, it was shown in the research that decreasing of the adsorbent capacity in case of single component occurs in the following sequence: from fructose to glucose.

1.5 Batch, SMB and SSR chromatography

The commonly equipment for *the batch chromatography* includes the reservoir with eluent, which is pumped through the column from where the products collecting occurs by switching fractionation valve. The process of chromatography usually assumes that the mobile phase composition stays constant during the separation, but in some cases gradient operation can be applied (Aniceto and Silva, 1238-1239).

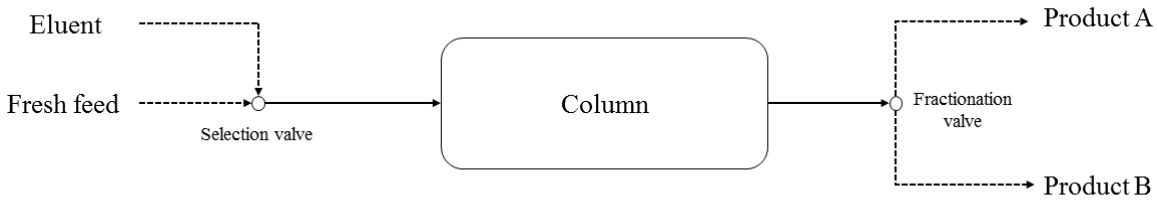

Figure 1.11. The scheme of batch chromatography (Siitonen and Sainio 2015, 438).

On the Fig. 1.11 schematic setup of batch chromatography is presented. The feed of eluent (E) is introduced continuously during the process. At certain time the fresh feed (FF)

begins to flow to the column by switching the selection valve. After feeding a predetermined volume of FF, the valve is returned to initial position – the feeding of E and the solutes spread via the column with various rates. The products of separation out from the column and divided by the fractionation valve in different reservoirs (Siitonen 2014, 20-21).

There are two strategies with given purities of separation of a binary mixture (components A and B), which are implied of essentially various operation and collection of the products (see Fig. 1.12). The first (I) strategy uses high column overloading and targeted to minimization of eluent consumption or high productivity. In order to fulfill the given purity of the separation, the collecting of the products proceeds only from the rear (t_{B2}-t_{B1}) and the front (t_{A2}-t_{A1}) parts of the chromatogram, while the other part (t_{B1}-t_{A2}), which is mixed of two solutes, is considered as waste or for further recycling. For the second (II) strategy the formation of the mixed part is not allowed. Therefore, with given purities the two products can be separated only by one cut (t_{A2}= t_{B1}) and, thus, the overload of the column is limited. During the design of the chromatography separation with strategy II, the primary purpose is to find the suitable parameters of the cut times and the pulse volume. For batch chromatography there are different optimization and design methods. Most of them use the first strategy, which has the higher productivity than the second because of no limitation of yield, otherwise, the second strategy is applied (Siitonen et al. 2013, 55).

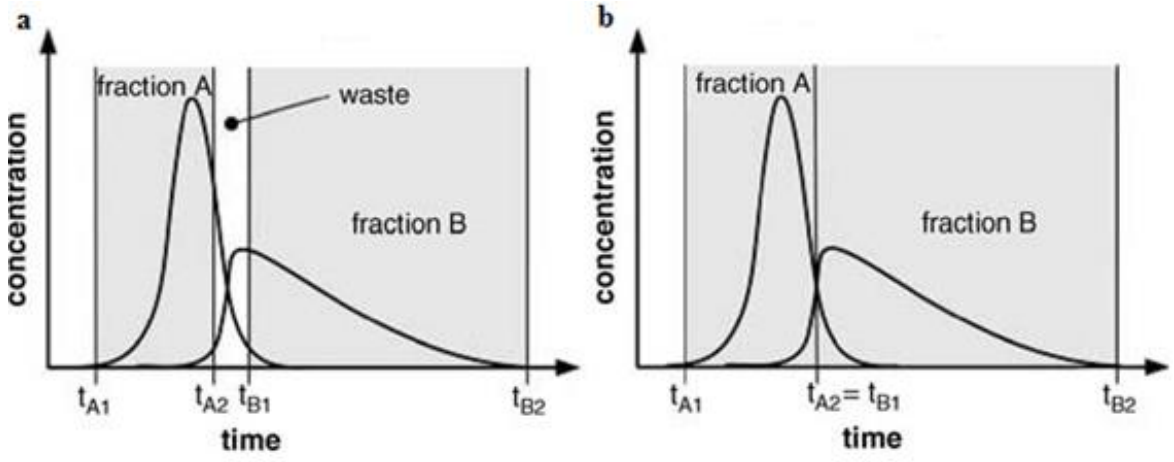

Figure 1.12. The chromatograms of separation of A and B components with applying first (a) and second (b) cut strategies (Schmidt-Traub et al. 2012, 443). The cut times, t_{A1}, t_{A2}, represent the beginning and the end of collection of the product A; t_{B1}, t_{B2} are the beginning and the end of product B collection.

The equipment for *the steady state recycling chromatography* (SSR) is the same as batch chromatography, but with recycle step and additional feed reservoir. The separation process is carried out in isocratic mode.

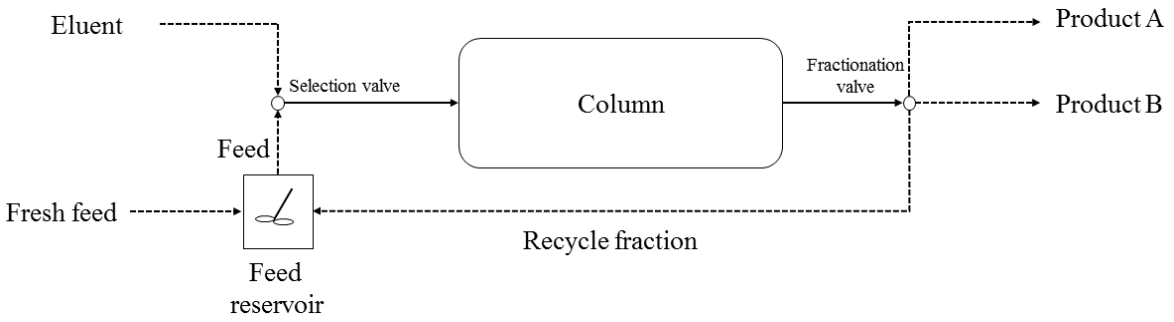

Figure 1.13. The scheme of SSR chromatography (Siitonen and Sainio 2015, 438).

On the Fig. 1.13 the scheme of steady state recycling chromatography is presented. Into an uncontaminated column the defined amount of mixture to be separated is entered from the feed reservoir (FR). Then selection valve is returned to another position – the feeding of E. The feed reservoir may contain a mixture of FF, a diluted mixture of FF or a solution with steady state feed compound (Siitonen and Sainio 2014, 16). The same process of separation and collection of fractions is performed as for the batch chromatography with using strategy I (Fig 1.12 (a)). The mixed part here is recycled as recycle fraction. The fractionation is made by corresponding valve.

In the mixed-recycle mode, the fraction to be recycled goes to the FR, where it is mixed with FF and then injected to the chromatographic column. A periodic steady state occurs when the above mentioned operations are repeated. This state means that concentration of the feed in column, band profiles and the average composition of the products become almost constant in all subsequent cycles (Siitonen 2014, 21).

The true moving bed (TMB) concept found its own practical application in *simulated moving bed* (SMB) chromatography. The latter imitates true moving bed process and devoid of the disadvantages associated with stability of the solid phase by simulating the adsorbent moving (Aniceto and Silva, 1246-1250). This is reached by the replacement of the column of true moving bed process by few another columns, which are smaller and have fixed solid bed, and changing the inlet and outlet streams at certain time step in the orientation of mobile phase motion.

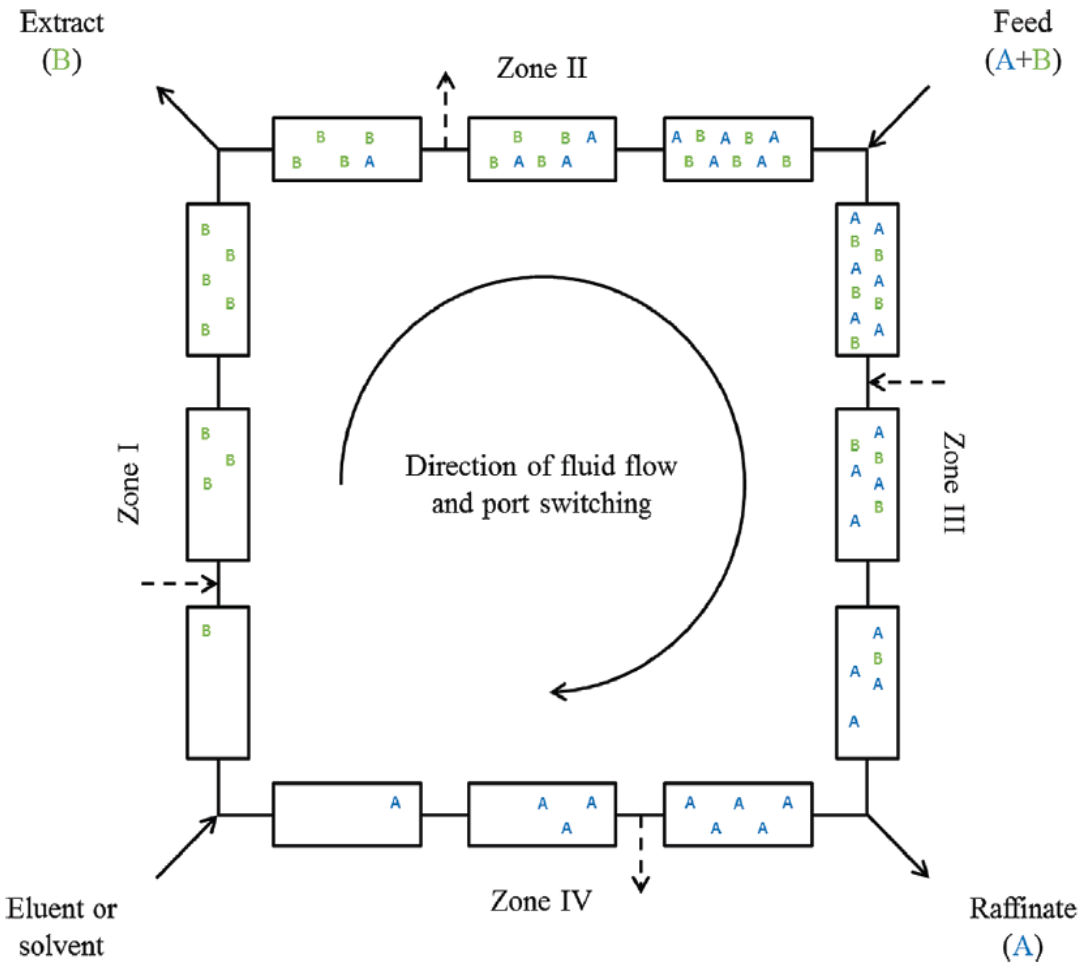

Figure 1.14. The scheme of SMB chromatography (Aniceto and Silva, 1248).

On the Fig. 1.14, the scheme of SMB chromatography is presented. There is specified column configuration which each of the four separation zones consists three small columns. In addition, there are four streams (two inlet and two outlet) which have the appropriate ports for injecting and for withdrawing.

The inlet streams are eluent and feed and the outlet streams are extract (B) and raffinate (A). The stream with compound which has higher retention factor (RF) and, thus, it is late eluted is called extract. Another stream with component that has lower RF and, therefore, it is early eluted, is called raffinate.

The separation on SMB system requires accurate control of the pumps both for achieving a constant inlet/outlet flow rates (4 streams) and for constant fluid mass in the column unit.

There are four different zones with certain role, which are divided by the inlet streams position in every certain period of time:

- First zone – the regeneration of the stationary phase or, in other words, component B desorption;
- Second zone – component A desorption;
- Third zone – component B adsorption;
- Fourth zone – the regeneration of the eluent or, in other words, adsorption of the component A.

The arrow, which is in the center of the scheme (see Fig. 1.14), represents the direction of the displacement of positions of the inlet and outlet ports which occurs every switch time interval - t^*, in seconds. This special parameter is essential for the design to get high productivity and purity of the separation process by SMB.

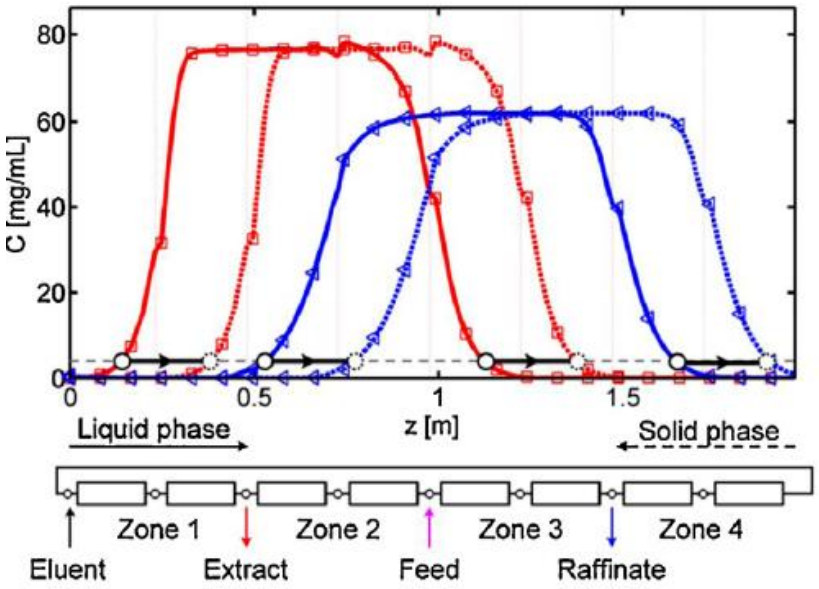

Figure 1.15. The chromatograms of fructo-oligosaccharides separation, carried out at cyclic steady state inside the SMB (Suvarov et al. 2014, 359).

The concentration profiles, obtained from SMB separation, are presented in Fig. 1.15. The process of separation was carried out in eight columns (Suvarov et al. 2014, 357-359). The movement of solid phase relative to mobile phase is counter-current, so the columns were rotated in the opposite direction to the flow of mobile phase. The black line with arrow represents the deviation from the initial position (solid line) to the end position (dotted line). To stabilize this movement to designed position, the cycle time and the external flow rate can be adjusted.

1.6 Unified Design method for chromatography

In order to apply SMB chromatography for separation of binary mixtures, a number of conditions should be fulfilled. The flow rates, Q_i, and switch time interval, t^*, must be thoughtfully chosen in every zone to obtain desired purity of the products. As it was mentioned before, SMB process is a practical application of TMB concept, where the volumetric flow rate of the adsorbent, Q_S, is correlated to t^* of the SMB unit by the following equation:

$$Q_s = (1-\varepsilon)A_{col}u_s = (1-\varepsilon)A_{col}L_c / t^* \tag{1.31}$$

where A_{col} is the column cross section, u_s is the apparent velocity of the adsorbent.

To determine the flow rate of mobile phase in TMB unit the next relationship is used:

$$Q_j^{TMB} = Q_j^{SMB} - Q_s / F \tag{1.32}$$

where Q_j^{SMB} and Q_j^{TMB} are the volumetric flow rates in SMB and TMB unit, respectively.

To provide a more simple method for design of simulated moving bed the triangle theory was formulated (Storti et al. 1993). The authors of this theory accounted for the effect of the various mobile phase velocities in the different zones of SMB on the specified separation requirements in ideal conditions (without taking into account axial dispersion and MTR). The key parameters of the triangle method are m_j - operational parameters, which are related to four sections of TMB and can be transformed to equivalent SMB. These parameters are the ratios between the net fluid (Q_j^{TMB}) and the adsorbent flow rates in each zone j, which is equal to section number from 1 to 4. The definition of m_j can be expressed by:

$$m_j = \frac{Q_j^{TMB}}{Q_s} \tag{1.33}$$

Taking into account the Eqs. 1.32 and 1.33, the operating parameters could be derived for the equivalent SMB unit:

$$m_j = \frac{Q_j^{SMB}}{Q_s} - \frac{1}{F} = \frac{Q_j^{SMB}t^* - V\varepsilon}{V(1-\varepsilon)} \tag{1.34}$$

In this theory, it was established that complete separation occurs only with specific combinations of operating parameters and, as a consequence, the specific conditions were

derived for such separation. The constraints suppose that the net flow rate of components must be negative for B and positive for A in second and third sections, and conversely (positive B and negative A) for first and fourth sections.

The complete separation of two components in case of linear isotherm is achieved subject to the following requirements (Storti et al. 1993, 473):

$$H_2 < m_1 < \infty \tag{1.35}$$

$$H_1 < m_2 < H_2 \tag{1.36}$$

$$H_1 < m_3 < H_2 \tag{1.37}$$

$$\frac{-\varepsilon_p}{1-\varepsilon_p} < m_4 < H_1 \tag{1.38}$$

With these specific conditions and corresponding coordinates, m_j , the four-dimension region is determined. Therefore, the operating conditions for complete separation could be obtained from the points of this space. The generally separation of the components is performed in second and third sections of TMB unit. As it was discussed above, the net flow rate in these sections is matches the expression $m_3 > m_2$ and, after combining it with Eqs. 1.36 and 1.37, the constraints become as:

$$H_1 < m_2 < m_3 < H_2$$

Due to this, the four-dimension space is transformed into the two-dimension (m_2, m_3) region, which is shown on Fig. 1.16. The triangle method, which is represented by this plane, is applied for determination of the operating conditions for SMB design.

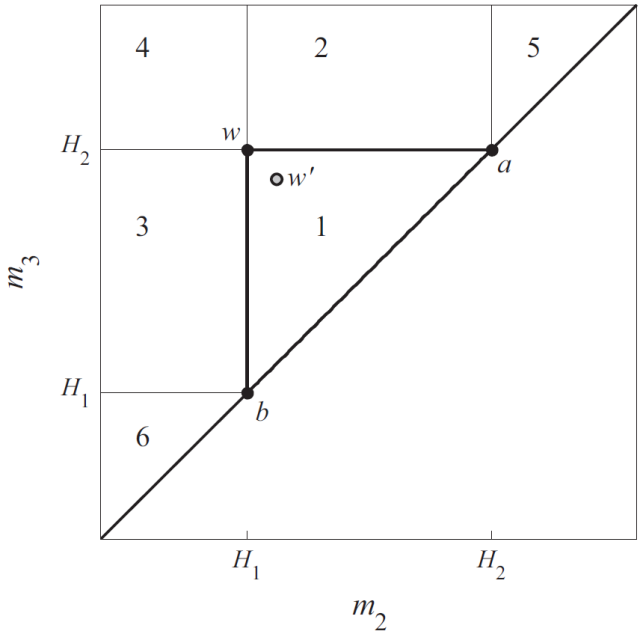

Figure 1.16. The separation regions under linear conditions based on m_2, m_3 constraints (Siitonen and Sainio 2015, 441).

Assume that the separation between compounds A and B takes place, then, there are 6 product regions which have the corresponding definition:

- 1 – triangle-shaped region, where complete separation and 100% purities for products of components A and B are achieved;
- 2 – region, where the pure product B is achieved and product A is polluted by B. The last occurs due to the fact that component B is not retained sufficiently (the constraint $m_3 < H_2$ is not fulfilled), transported forward and contaminates A;
- 3 – region, where the pure product A is achieved and product B is polluted by A. It happens due to the same reason as for region 2, but now the constraint $m_2 > H_1$ is not fulfilled;
- 4 – region, where $m_3 > H_2$ and $m_2 < H_1$, therefore, the contamination of both products is;
- 5 – region, where B is flooded with the eluent and A is flooded with FF – no separation, because $m_3 > H_2$ and $m_2 > H_2$;
- 6 – region, where A is flooded with the eluent and B is flooded with FF - no separation, because $m_3 < H_1$ and $m_2 < H_1$.

As the application of triangle method for the SMB design has proven extremely useful, its further development is reflected in *Unified Design* of chromatographic processes (Siitonen

and Sainio 2015). The example will be given for the classical batch chromatography for linear isotherm under ideal conditions.

There are 5 operating parameters for batch, which are freely adjustable: $\Delta\tau_F$ is the duration of feed injection; τ_{A1} , τ_{A2} are the beginning and the end of collection of the product A, respectively; $\tau_{B1} = \tau_{A2}$ (no recycling stream), τ_{B2} are the beginning and the end of product B collection and $Q = \varepsilon A_{col} u^L$ is the fluid phase volumetric flow rate; - and can be written as:

$$\Delta\tau_F = F(m_3^{batch} - m_2^{batch}) \tag{1.39}$$

$$\tau_{A1} = Fm_4^{batch} + 1 \tag{1.40}$$

$$\tau_{A2} = \tau_{B1} = Fm_3^{batch} + 1 \tag{1.41}$$

$$\tau_{B2} = Fm_1^{batch} + 1 + \Delta\tau_F \tag{1.42}$$

$$\Delta\tau_{cycle} = \tau_{B2} - \tau_{A1} \tag{1.43}$$

Each m_j^{batch} characterizes the difference between eluted mobile phase volume from the column before a given cut point and mobile phase volume in the column compared with stationary phase volume.

Due to the fact that the component (i = 1, 2) velocity for linear isotherm not depends on concentration, the retention, τ_{Ri}, and elution, τ_{Ei}, times can be defined as:

$$\tau_{\mathrm{Ri}} = 1 + FH_i \tag{1.44}$$

$$\tau_{\mathrm{Ei}} = 1 + FH_i + \Delta\tau_F \tag{1.45}$$

It is necessary to define the constraints for cut times:

$$\tau_{A1} \le \tau_{R1} \tag{1.46}$$

$$\tau_{R2} \ge \tau_{A2} = \tau_{B1} \ge \tau_{E1} \tag{1.47}$$

$$\tau_{B2} \ge \tau_{E2} \tag{1.48}$$

$$\Delta\tau_F > 0 \tag{1.49}$$

After replacing equations 1.39-1.43 and 1.44-1.45 in Eqs. 1.46-1.49, the new constraints were obtained and expressed by:

$$H_2 \le m_1^{batch} \tag{1.50}$$

$$H_1 \le m_2^{batch} \le m_3^{batch} \le H_2 \tag{1.51}$$

$$m_4^{batch} \le H_1 \tag{1.52}$$

It was determined that the constraints of m-parameters for classical batch chromatography are the same as for SMB. This statement implies that the maximum FF quantity that can be operated during a cycle in batch chromatography is identical to that in the SMB chromatography during a switch (Siitonen and Sainio 2015, 441). Therefore, the two-dimension plane for designing SMB process is also suitable for batch process.

In addition, it was shown that the constraints are also the same for other processes (or systems with Langmuir isotherm). For SMB, SSR and batch chromatography, the four dimensionless parameters $(m_1 - m_4)$ were derived. For cross-current and steady state recycling systems, recycling provides additional operating parameter - m_R. These parameters are presented in Table 1.1 (Siitonen and Sainio 2015, 440).

Table 1.1. The operating parameters for different processes.

Net flow rate	TMB	SMB	Batch and SSR
m_1	$\frac{Q_1^{TMB}}{Q_s}$	$\frac{Q_1^{SMB}t^* - V\varepsilon}{V(1-\varepsilon)}$	$\frac{Q(t_{B2} - \Delta t_F) - V\varepsilon}{V(1-\varepsilon)} = \frac{\tau_{B2} - \Delta\tau_F - 1}{F}$
m_2	$\frac{Q_2^{TMB}}{Q_s}$	$\frac{Q_2^{SMB}t^* - V\varepsilon}{V(1-\varepsilon)}$	$\frac{Q(t_{B1} - \Delta t_F) - V\varepsilon}{V(1-\varepsilon)} = \frac{\tau_{B1} - \Delta\tau_F - 1}{F}$
m_3	$\frac{Q_3^{TMB}}{Q_s}$	$\frac{Q_3^{SMB}t^* - V\varepsilon}{V(1-\varepsilon)}$	$\frac{Qt_{A2} - V\varepsilon}{V(1-\varepsilon)} = \frac{\tau_{A2} - 1}{F}$
m_4	$\frac{Q_4^{TMB}}{Q_s}$	$\frac{Q_4^{SMB}t^* - V\varepsilon}{V(1-\varepsilon)}$	$\frac{Qt_{A1} - V\varepsilon}{V(1-\varepsilon)} = \frac{\tau_{A1} - 1}{F}$
m_R			$\frac{V_R}{V(1-\varepsilon)} = \frac{\tau_{B1} - \tau_{A2}}{F}$

1.7 Techniques for separation of carbohydrates and their industrial application

For the industrial separation of carbohydrates there are some techniques that are used, where the most widely applied is chromatographic separation.

One of the way to separate glucose and fructose from their mixtures is using of ionic liquids (selective solvents). This approach can be carried out at various temperatures. The solubility of sugars in these liquids mostly depends on the type of anion used in ionic

liquids. The experiments were carried out with several type of the anion and, therefore, different dissolution of the fructose or glucose were achieved. The process of sugar separation consists of using ionic liquids, dissolution of the component and then filtration for further separation of deposited sugar. The separation from ionic liquids is carried out in centrifuge by extraction of water. The sugars recovery was reached the point under 90% and the separated sugar has 99% of purity (Hadj-Kali and AlNashef 2015, 417-421).

Another separation method of model carbohydrates solution were made by nanofiltration. This method can be applied in industry for fructans separation and concentration from natural mixtures of carbohydrates. It was presented that with using a pilot cross-flow unit with special selected membrane the separation can be done between different carbohydrates with various molecular weight. It was shown that rejection of inulin can be achieved over 90% with applicable operating conditions from sugars with low molecular weight, i.e. fructose, sucrose and glucose (Moreno-Vilet et al. 2014, 84-85, 92-93).

Alternate way to separate carbohydrates (glucose-maltose) is a using of system of moving U-shaped column. It includes 12 columns with U-shape form, which are suspended from the main unit. The columns were connected to the rotating part of the main cylinder, which contained the inlet, outlet, and interconnecting channels. This design approach permits column movement and effects a countercurrent flow between the packing material (potassium form ion-exchange resin with 50-100 μm particles) and the mobile phase by employing only one stationary rotational interface. The 90% purity was achieved in this separation equipment and 99% were found to be possible. But problems with stationary phase maintenance and uniform packing efficiency have limited its widely application in preparative scale (Ganetsos and Barker (ed.) 1993, 180-185).

In case of semicontinuous chromatographic refiner (or SCCR) with anion-exchange resin in HSO_3^- for separation of glucose and fructose (desired product) could be used as advantageous technique, because of strong retaining of glucose (Ganetsos and Barker (ed.) 1993, 245-254). However, with multicomponent carbohydrate feed, fructose separation cannot be achieved in single pass due to the poor purity. Also, this type of resin suffer from auto-oxidation brought about by the dissolved oxygen in the eluent. That is why anion-exchange resins are not applied in large-scale production and in industrial high-fructose corn syrups producing systems employed mainly cation exchangers (polystyrene resins in Ca^{2+} form).

The chromatographic separation (c.s.) of carbohydrates can be also applied for tagatose manufacturing (Bertelsen et al. 2006) where it is designed for recycling of lactose and galactose for further processing.

The simulated moving-bed process is a beneficial technique with comparison to moving-bed process. SMB shows almost the same performance as MB and it does not have difficulties related with breaking resins during separation in consequence of friction among particles and do not flow uniformly in the column. It was applied in many fields such as hydrocarbons separation, producing of high-fructose sugar and some pharmaceutical applications.

The examples of some industrial chromatographic separation processes would be presented below.

The fructose and glucose separation is a widely known process because its products are widely used in the food-manufacturing industry (A. Khosravanipour Mostafazadeha et al. 2011, 72). The general scheme (see Fig. 1.17) shows the main steps of corn sweetener processing and types of resins that are utilized (Dow 2010).

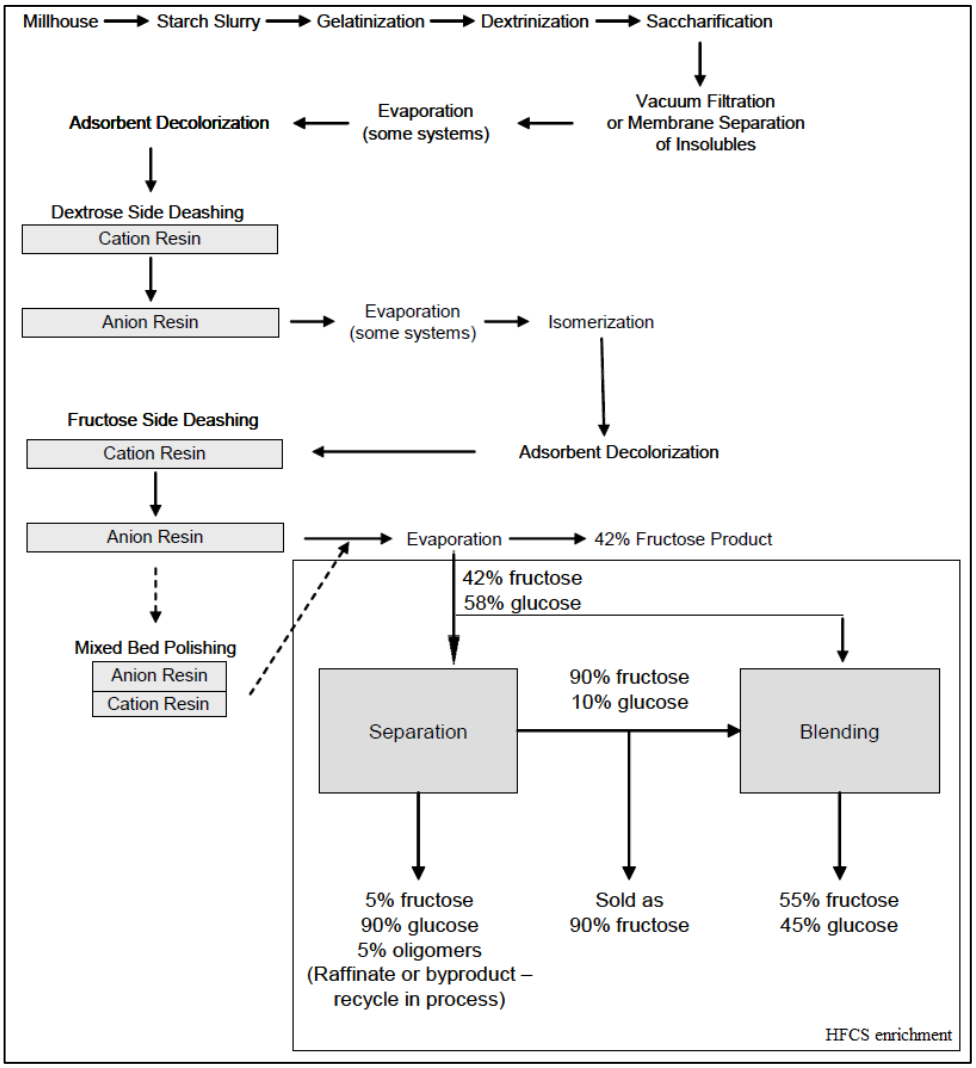

Figure 1.17. The general scheme of corn sweetener processing (Dow 2010).

With using traditional processes and because of economically limitation, only 42% of fructose conversion is possible. To increase it up to 55% (and obtain high fructose corn syrup - HFCS), the SMB chromatography separation is applied, from where 90% concentrations of fructose and glucose streams are achieved. The high purity fructose is then blended with 42% stream to get a final HFCS product.

Another example is devoted to industrial multi-step chromatographic separation of different monosaccharides (Saari 2011, 50-51), where different types of resins are used to enhance the final purities (Q, %) of the product (see Fig. 1.18). However, the processes are not complete and should contain additional operations, such as: purification, filtration, ion exchange and others.

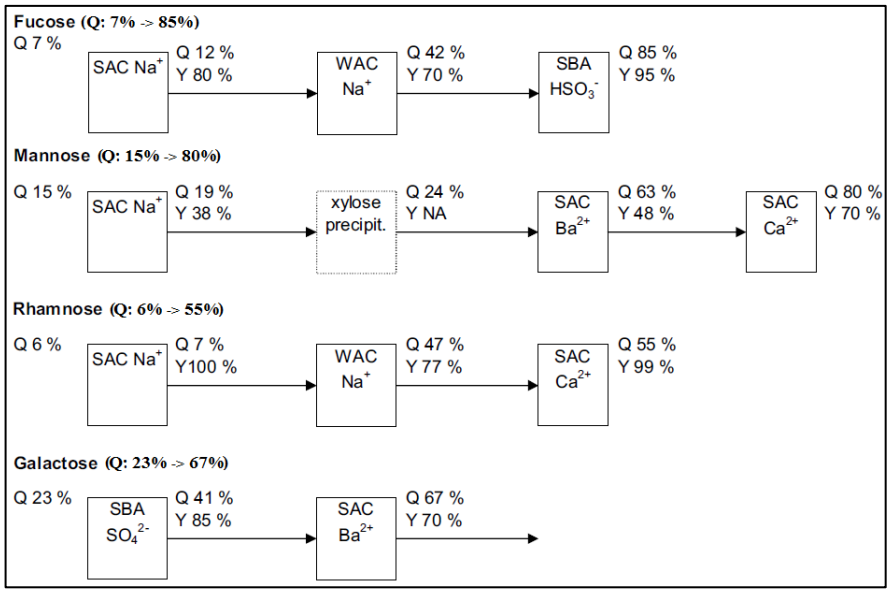

Figure 1.18. Industrial multi-step chromatographic separation of monosaccharides. Y – the product yield, % (Saari 2011, 51).

The technological scheme for large scale production of L-fucose was proposed by Pia Saari (Fig. 1.19). The spent sulfite liquor was introduced as a raw material for separation process. The application of three chromatographic columns with different resins allows removing oxidizing agents, which disturbs equipment work, and achieving the purity of fucose from 7% to 85%.

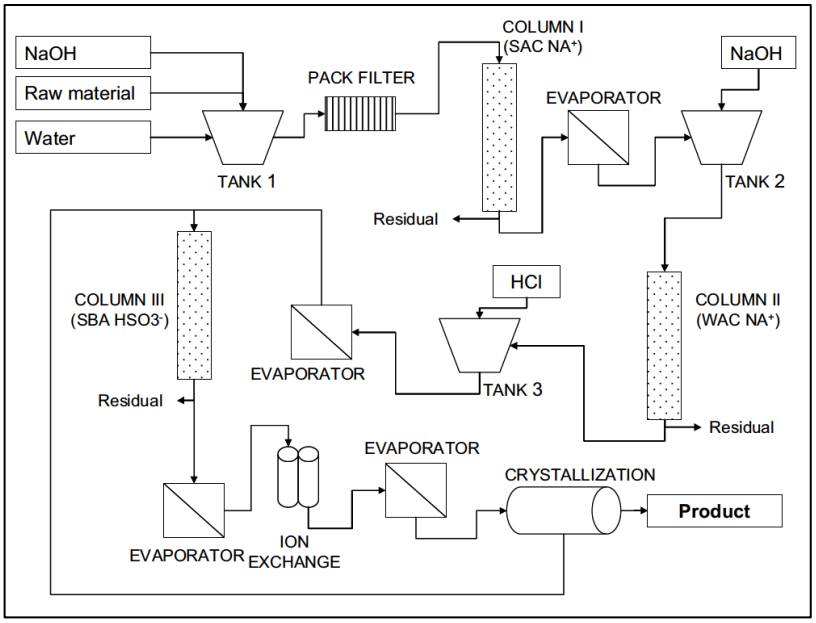

Figure 1.19. The technological scheme for L-fucose production (Saari 2011, 55).

2. APPLIED PART

In order to understand and describe the influence of column efficiency on the region of feasible operating parameters the number of simulations were made with using special software MATLAB, which is designed and programmed by Tuomo Sainio. The program allows carrying out experiments for batch and SSR chromatography under ideal and non-ideal conditions by setting the corresponding parameters. The results of the simulations are presented in the form of the figure with separation chromatogram and data, which could be extracted for further processing.

2.1 Batch mode simulations for Dowex Monosphere 99/Ca gel type resin

The batch mode simulations of chromatographic separation were made for 2 components: glucose and fructose; with total concentration – 200 g/L. As it was mentioned before (see Chapter 1, Section 1.4.3), the equilibrium isotherms for these components are linearly dependent for a wide range of concentrations and, thus, the Henry constants of adsorption isotherms for Dowex Monosphere 99/Ca strong acid cation gel type resin in Ca^{2+} form were used (A. Khosravanipour Mostafazadeha et al. 2011, 77). To obtain more realistic and close to practical results, the simulations were carried out with taking into account non-ideal conditions: the influence of axial dispersion and mass transfer resistance (more detailed in Chapter 1, Section 1.3) by setting the corresponding parameters. The procedure of the simulations is given below.

At the first step, the initial parameters of simulation, which are constant during experiments, were set and they are presented in Table 2.1.

Table 2.1. The parameters of the simulation.

The name of parameter	The value of parameter	
The column parameters		
Height, m	0.7	
Diameter, m	0.015	
Volume, ml (V)	120	
Bed porosity (ε)	0.4	
The component parameters		
	Glucose (A)	Fructose (B)
The concentration, g/L	116	84
The Henry constant	0.29	0.63

It was assumed to make simulation for the purities of components 90%. For this value, the plots were achieved with high enough domain of feasible operating parameters. Then the intraparticle diffusion coefficient was taken for both components as $1 \cdot 10^{-9}$ m^2/s, particle

size d_p = $280 \cdot 10^{-6}$ m and the flow rate Q = 4 ml/min. With the first simulation the pulse size was assumed as 1%.

After running the program, data, which contains the results, was retrieved from the "outlet.dat" file. This data contains time and time dependent values of the components concentrations.

The purity of components was calculated by already mentioned equation (see Chapter 1, Section 1.1.3):

$$P_i^j = \frac{m_i^j}{m_1^j + m_2^j} \cdot 100, \ \% \tag{2.1}$$

The cut time for considered purity value (90%) was extracted and for the first component it was 21.6508 min (t_{A2}) and for the second - 20.4092 min (t_{B1}).

The number of theoretical plates was obtained by using Eq. 2.2 (Tsarev et al. 2000, 126).

$$N_i = 5.55\left(\frac{t_{R,i}}{w_{1/2,i}}\right)^2 \tag{2.2}$$

The number of theoretical plates, N_i, for the components was calculated with using above-mentioned data and received for glucose $N_A = 112$, for fructose $N_B = 96$.

The next step is calculating operating parameters for this separation with using Eq. 2.3 and Eq. 2.4 (more detailed in Chapter 1, Section 1.6).

$$m_2 = \frac{Q(t_{B1} - \Delta t_F) - V\varepsilon}{V(1-\varepsilon)} \tag{2.3}$$

$$m_3 = \frac{Q t_{A2} - V\varepsilon}{V(1-\varepsilon)} \tag{2.4}$$

where Δt_F is the duration of feed pulse which is equal to $\frac{V}{Q} \cdot pulse\ size / 100$.

The operating parameters for the first experiment are 0.48351, 0.50017 for component A and 0.41659, 0.43326 for component B.

Then with changing the pulse size and performing previous steps, the region of feasible operating parameters was obtained (see Fig. 2.1). In this figure, the red solid line represent "ideal conditions" (infinite column efficiency) boundaries for 100% purity of both components, green solid line - "ideal conditions" for 90% purity and the domain under

green dashed lines – non-ideal for 90% purity. In the point of intersection of the green dashed, red and green solid lines the highest productivity is observed. Due to the influence of the axial dispersion, low separation factor and other parameters, this area becomes much smaller compared with the case of ideal conditions.

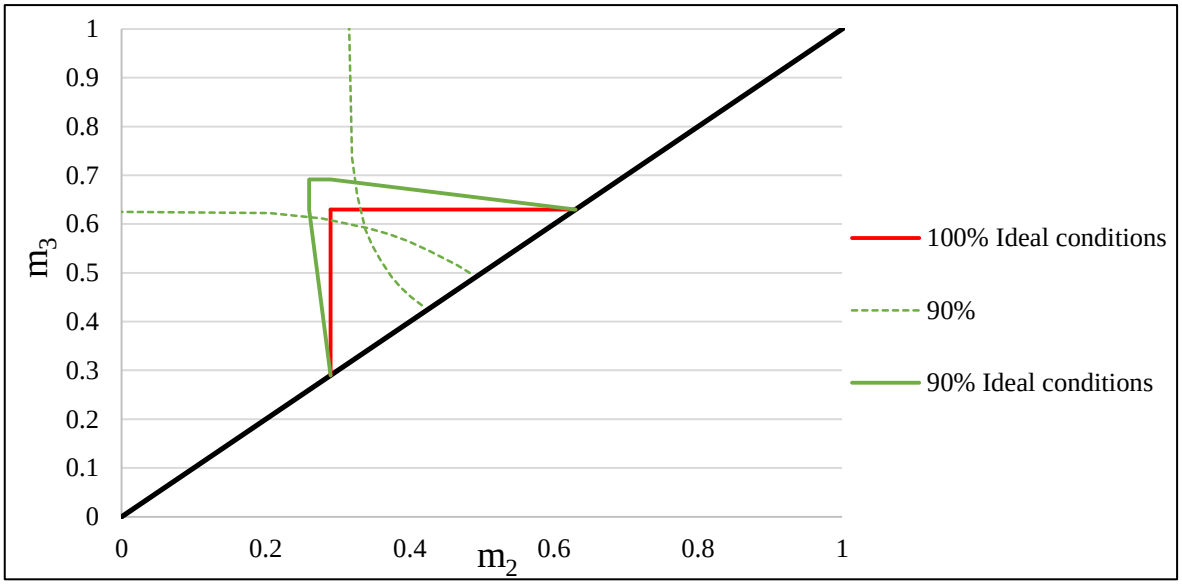

Figure 2.1. The obtained plot from the first simulation. Purity requirements are set to 90%, range of pulse size was used from 1% to 45% of the column volume.

To obtain the separation region under ideal conditions for SMB with purity lower than 100% the following equations were used (Rajendran et al. 2009, 717):

$$H^*_A = \frac{H_B c_B^F (P_R - 1) + H_A c_A^F P_R}{c_B^F (P_R - 1) + c_A^F P_R} \tag{2.5}$$

$$H^*_B = \frac{H_B c_B^F P_E + H_A c_A^F (P_E - 1)}{c_B^F P_E + c_A^F (P_E - 1)} \tag{2.6}$$

The utilizing of these equations applies to linear isotherms under restrictive case. This strategy implies that operating parameters m_1 and m_4 fulfill the constraints, given in Chapter 1, Section 1.6, and overlapping of the chromatograms not occurs. It was established in (Siitonen and Sainio 2015, 447-448) that boundaries of operating region under reduced purities and restrictive case are matched for SSR and batch process and, with using Unified Design method, could be matched for SMB also (under the restrictive case and linear isotherms). Therefore, the above written equations could be used for obtaining the operating regions under ideal conditions for batch process.

By following previous steps, other simulations were made. The main purpose of them was to investigate what kind of regions can be obtained with higher efficiency of the column.

For increasing N value, the next parameters were changed: the intraparticle diffusion coefficient, the particle size and the flow rate. Their values are presented in Table 2.2.

Table 2.2. The parameter values in different simulations.

The name of parameter	The value
The second simulation	
The intraparticle diffusion coefficient, D_{pore}, m^2/s	$1 \cdot 10^{-8}$
The particle size, d_p, m	$280 \cdot 10^{-6}$
The flow rate, Q, ml/min	4
The number of theoretical plates for A / B component respectively, N_i	426 / 407
The third simulation	
The intraparticle diffusion coefficient, D_{pore}, m^2/s	$1 \cdot 10^{-8}$
The particle size, d_p, m	$160 \cdot 10^{-6}$
The flow rate, Q, ml/min	4
The number of theoretical plates for A and B component respectively, N_i	855 / 825
The fourth simulation	
The intraparticle diffusion coefficient, D_{pore}, m^2/s	$1 \cdot 10^{-8}$
The particle size, d_p, m	$160 \cdot 10^{-6}$
The flow rate, Q, ml/min	2.4
The number of theoretical plates for A and B component respectively, N_i	915 / 872

The obtained operating regions for four experiments are presented in Fig. 2.2.

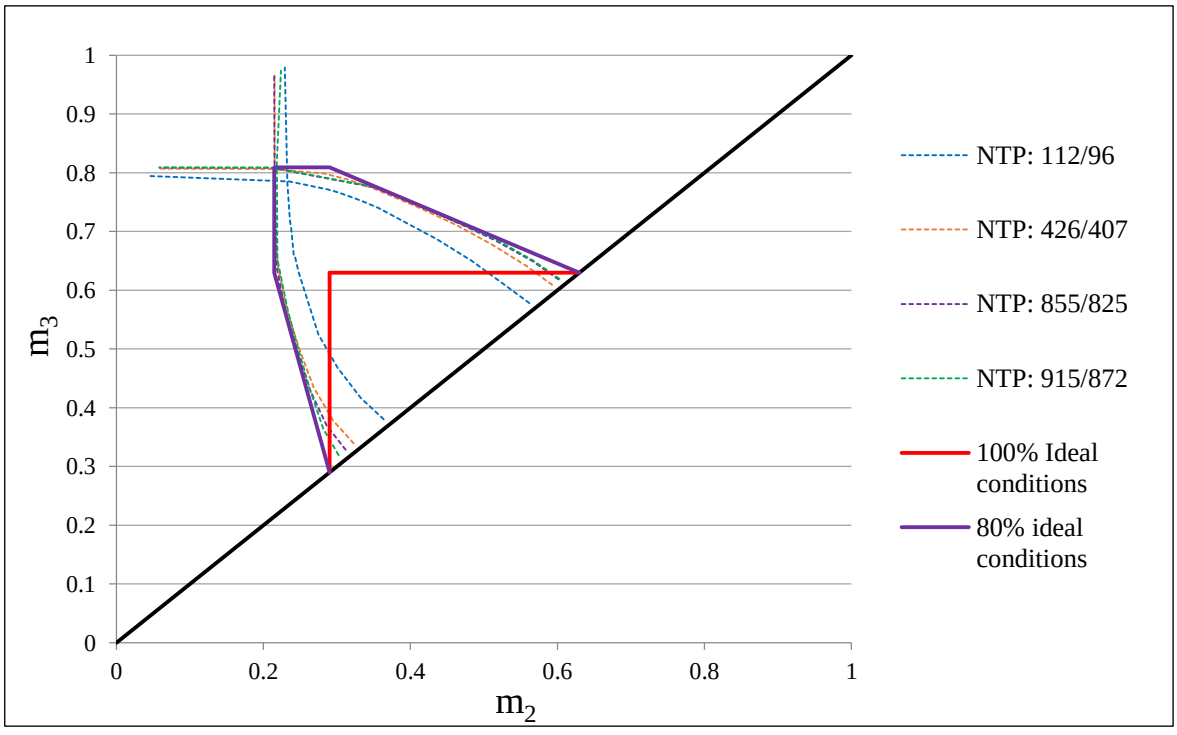

Figure 2.2. The dependence of the area of operating parameter space from the efficiency of the column. Purity of the components is set to 80%.

From the Fig. 2.2, it is seen that with increasing efficiency (or number of theoretical plates - NTP) the area of the region of feasible operating parameters expands also. Moreover, the

maximum productivity is also increased: the point of intersection of dashed lines with same color rises higher with each increase of NTP. For example, the productivity for glucose and fructose separation with $N = 100$ is equal to (78.22 and 45.01) g/L(bed)/h, respectively, while with $N = 400$ it is (92.67 and 53.362) g/L(bed)/h. However, the step of increasing the maximum loading is decreased, presumably, after $N = 400$ and therefore, the further increasing of N is inexpedient. The pulse size is growing with the sequence from the first to the fourth simulations: 33% --> 35.8% --> 35.9% --> 35.9%. In addition, the growth of the area may occur with a certain dependence that could be derived, but it is challenging enough.

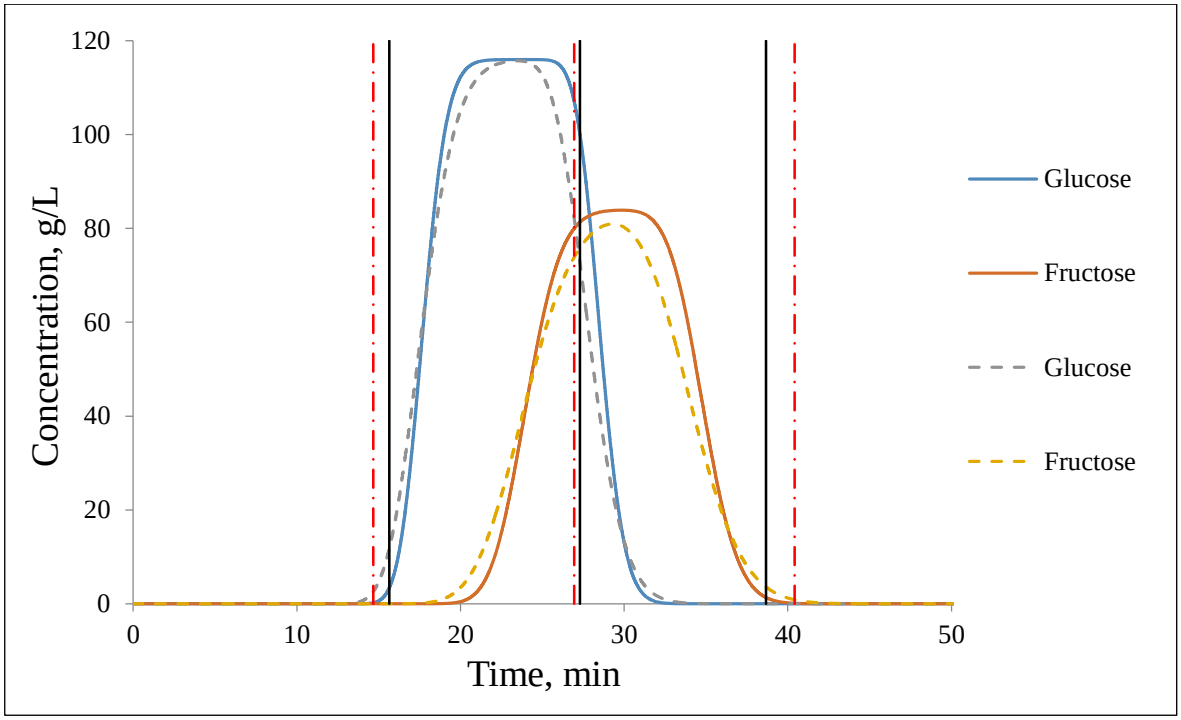

Figure 2.3. The chromatogram profiles of glucose and fructose separation. The dash-dotted line represents the case when $N = 100$ with corresponding cut times (vertical dash-dotted lines), the solid line: $N = 400$.

To give a perception of what kind of chromatograms at maximum productivity is obtained with increasing column efficiency, the Fig. 2.3 is demonstrated. Because of higher NTP and better separation, the loading of the column increases from 33% to 35%. The plateau region, which is appeared at $N = 400$ (due to the increased pulse size), characterizes the initial concentration of components and has impact on the cycle time of separation, which is decreased, and on the increasing of productivity.

The next step was to make additional sets of experiments with different values of purity of the components, which were selected as 90% and 99.9%. Keeping the above-mentioned

steps, the simulations were performed and resulting data is presented on the figures below. Other plots are presented in Appendix 1.

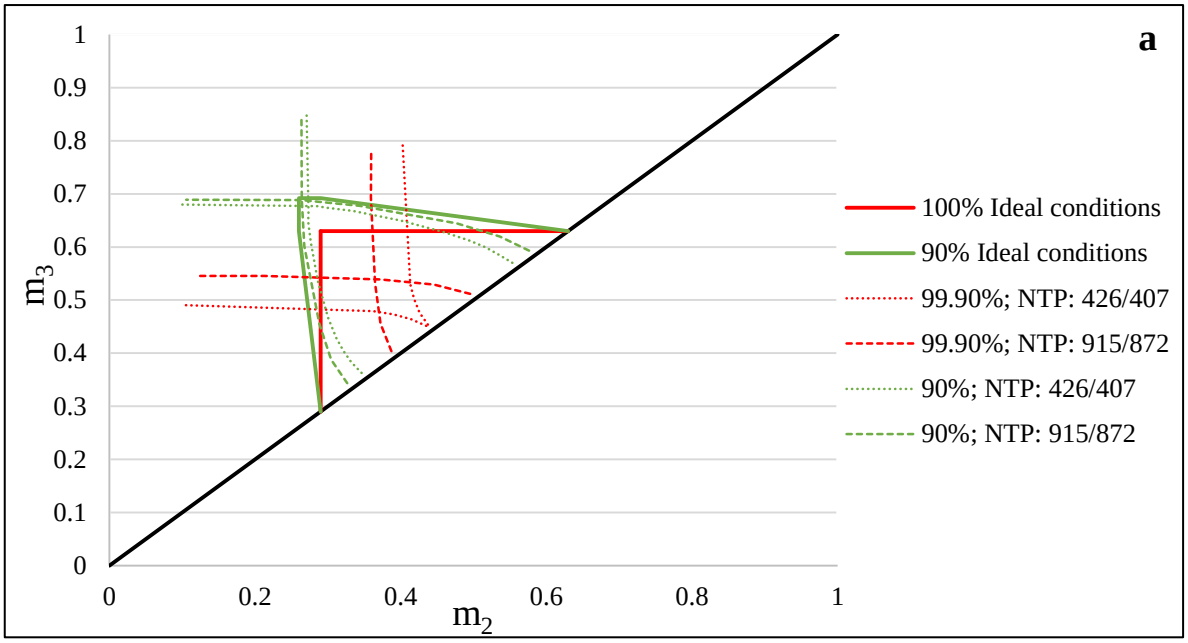

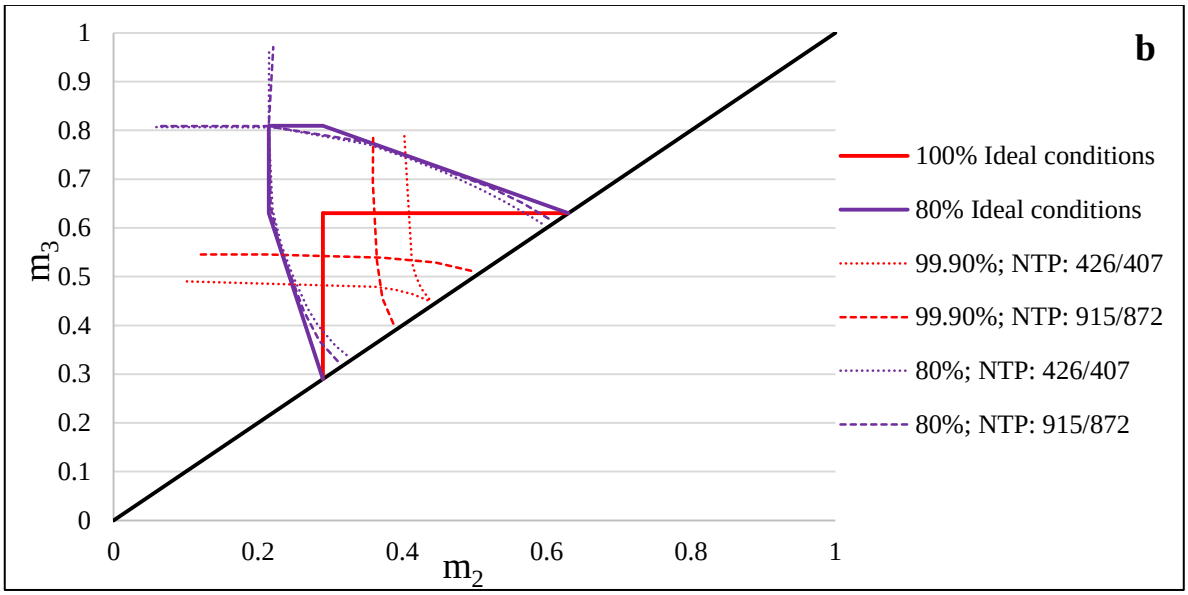

Figure 2.4. Effect of the increasing column efficiency (changing the particle size, d_p, from $280 \cdot 10^{-6}$ m to $160 \cdot 10^{-6}$ m and the flow rate, Q, from 4 ml/min to 2.4 ml/min) to the feasible operating region at 99.9% and 90% purity (a) and 99.9% and 80% purity (b) of fructose and glucose.

One can see that with N = 400 the complete separation for target purity of 99.9% cannot be achieved because of the very small operating region (see Fig. 2.4 (a)). However, when particle size was decreased, the efficiency of the column rises and the max pulse size, that can be used, is also increased (see Fig 2.4 (b)). From the further simulations, the shape of the area of operating parameters for this purity becomes more resembling as a triangle

(see Appendix 1). The another fact, which could be observed from previous figures, is that at some value of NTP the feasible operating parameter space at non-ideal conditions is close to be described by the boundaries of the region under ideal conditions. This may means that with certain number of theoretical plates and desired purity ($\approx$400 for 80% purity and $\approx$900 for 90% purity) the operating parameters for chromatographic separation process can be used from the case of ideal conditions. This fact is appeared for the first time and could be useful for simplification of separation process designing of batch, SSR or SMB chromatography with applying Unified Design method. Therefore, additional simulations are needed for more accurate determining the minimum NTP required to approach to the boundaries of ideal conditions and to use obtained operating region for process designing under non-i.c. as for the case of i.c. The simulations would be performed not only for 80% purity, but also for other target purities, which were taken as 90% and 99-99.9%.

2.1.1 Estimation of the minimum NTP for Dowex Monosphere 99/Ca gel type resin

For finding the minimum number of theoretical plates the sets of simulations were conducted. The parameters were set as it is presented in Table 2.1. The flow rate is equal to 4 mL/min.

First experiments were made for 80% purity both for glucose and for fructose and results are presented on Fig. 2.5. The number of theoretical plates was varied from 100 to 400. On closer inspection, it turned out that in this case the minimum value is 300 and it will be enough to correspond to the boundaries of ideal conditions. Moreover, further increase the column efficiency will not lead to significant changes. It will provide only small, gradual approach to the ideal case. Besides it, the operating points are always used near the center of the region but not the edges.

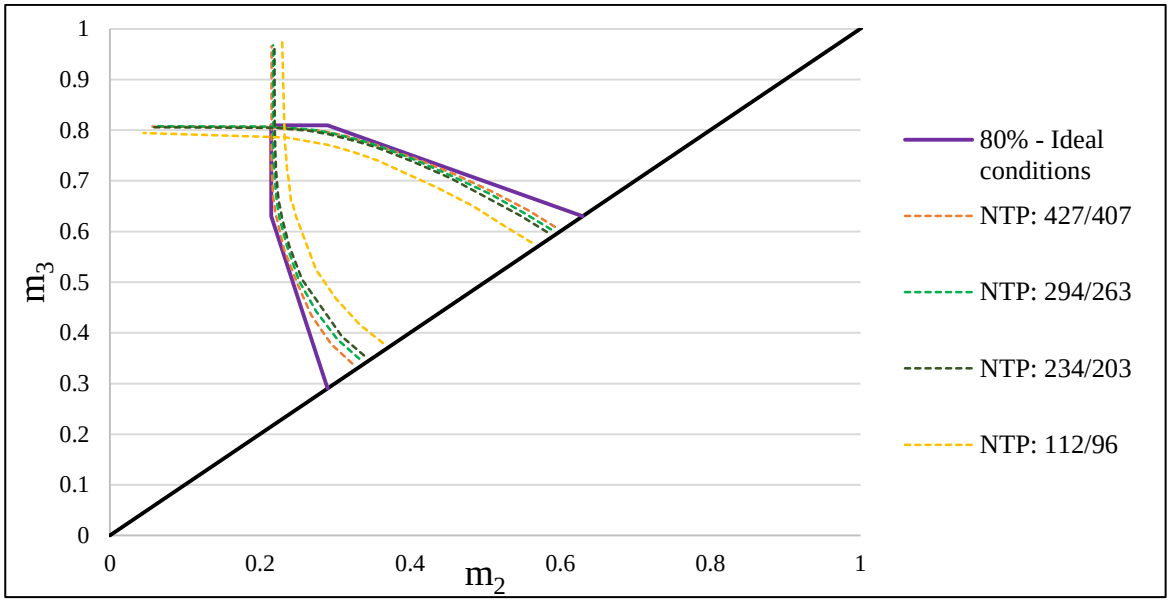

Figure 2.5. The changing of the area of operating parameter space from increasing number of theoretical plates in the column. Purity is set to 80%. The particle size varied from $280 \cdot 10^{-6}$ m to $160 \cdot 10^{-6}$ m and the intraparticle diffusion coefficient, D_{pore}, changed to $1 \cdot 10^{-8}$ m^2/s to obtain $N = 400$.

The second research was done for 90% purity and, as shown in the figure below, the NTP was ranged between 400 and 1500, where 900 was found as a minimum.

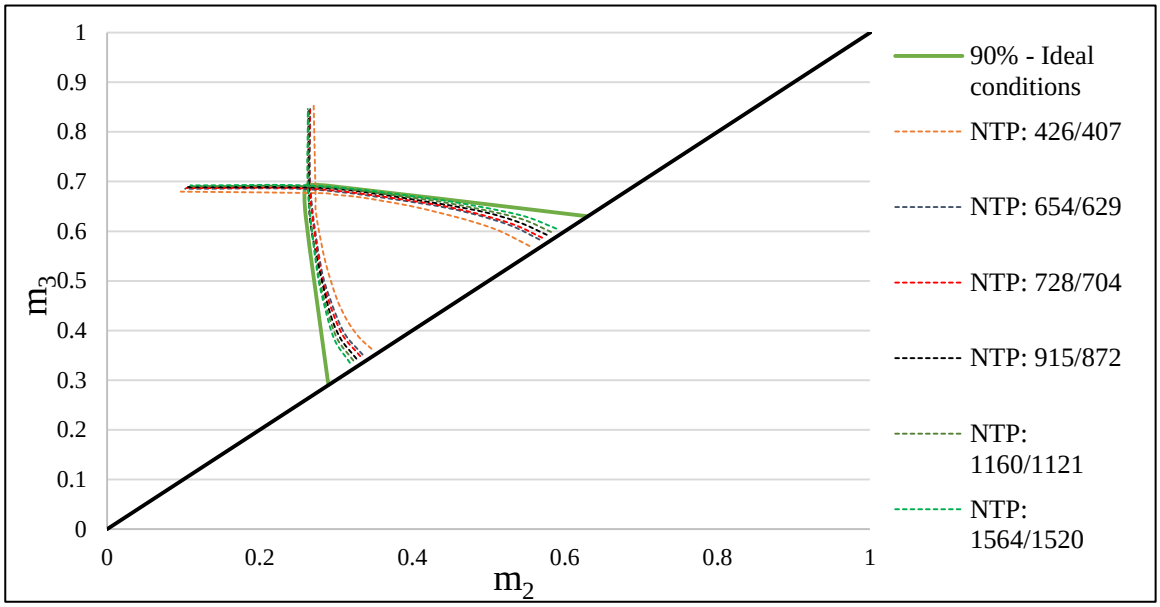

Figure 2.6. Influence of column efficiency on operating parameter space. The separated products have 90% purity. The intraparticle diffusion coefficient, D_{pore}, is equal to $1 \cdot 10^{-8}$ m^2/s and the diameter of the particle gradually decreased up to $90 \cdot 10^{-6}$ m.

The third observation was made for target purity 99.9%, which has been considered as 100% purity (see Fig. 2.7). To achieve pure products it is needed to have a chromatographic column with much higher efficiency. Therefore, range of NTP was varied

from 2 600 to 10 000. The minimum number of theoretical plates should be more than 9000. However, if the purity requirements decrease to 99% the situation is changed and it fulfills the region as for the 99% and 100% for the both components under ideal conditions.

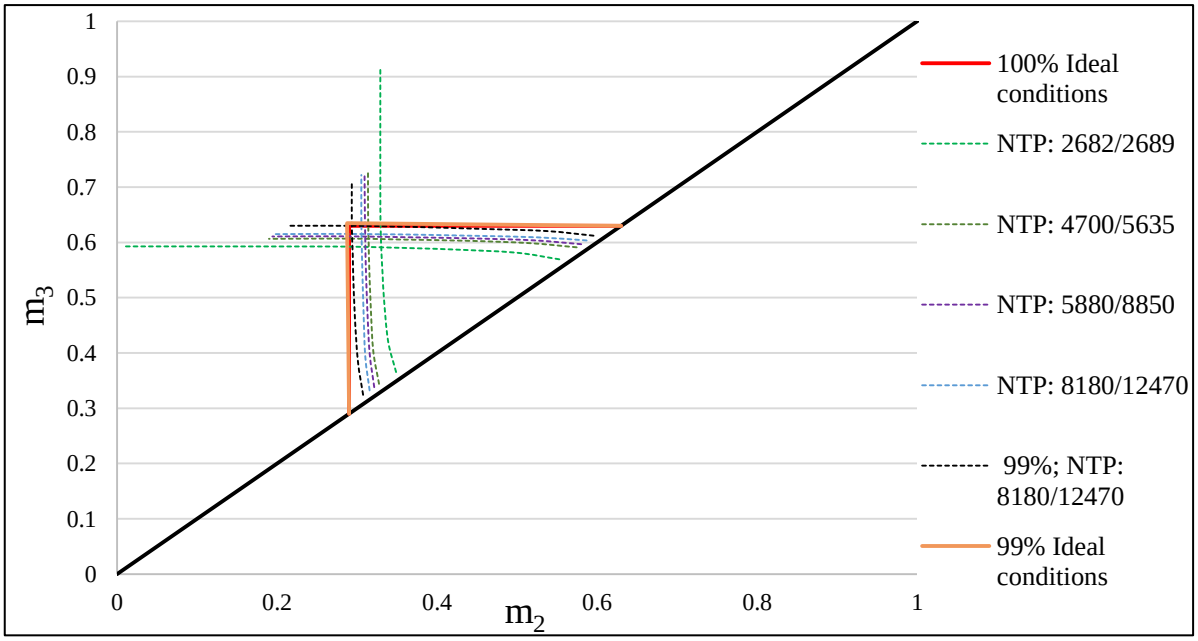

Figure 2.7. The results of simulations for obtaining boundaries of the operating regions at different NTP level. The target purity of the both products is set to 99.9% for all simulations and additionally to 99% for the last, with highest efficiency of the column.

2.2 Determination of the isotherm parameters for Finex CS11GC gel type resin

To compare obtained results with another resins, and consequently with the new Henry constants, the experiments with real column were carried out. The targets of the experiments are the determination of the parameters of isotherm for two components and defining the HETP values for a number of flow rates. In addition, they are needed for further validation and checking the proposed hypothesis.

The Figure 2.8 shows a simplified diagram of equipment for chromatography. The reservoir (or flask) contains the eluent (water), which is pumped through the column. The injector is needed to deliver feed at the certain concentration into the flow. The detector detects the substances when coming out of the column and transfers the data to computer. All the data obtained was exported to a text file.

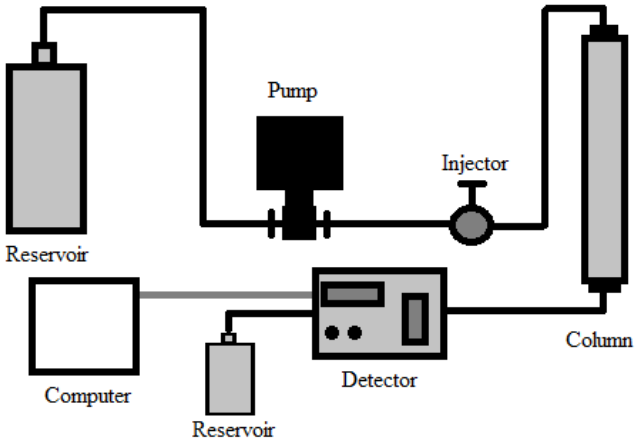

Figure 2.8. Simplified diagram of an equipment for chromatography

The column dimensions and resin type are presented in Table 2.3. The adsorbent was manufactured by Finex Oy in Kotka, Finland.

Table 2.3. The parameters of the laboratory equipment

The name of parameter	The value of parameter
The column parameters	
Height, m	0.685
Diameter, m	0.015
Volume, ml (V)	121.05
The resin parameters	
Name	Finex CS11GC in Ca^{2+} form
Type of the resin	Strong acid gel type cation exchange resin
The particle size, d_p, m	$250 \cdot 10^{-6}$

The chromatographic column was carefully packed, avoiding air bubbles formation, by mentioned resin. Before making the experiments, there are parameters that should be determined firstly: equipment void volume and porosity of the column. The first is needed to find the retention volume and, depends on the equipment used, it is different for refractive index and for ultra-violet detectors. The second is used in the calculation of the isotherms constants.

2.2.1 Defining of the column void volume

For determination of the column porosity blue dextran was used because its large nonbinding molecule does not interact with the resin. The refractive index detector was applied for molecules detection.

After launching pumping of the eluent through the column at flow rate Q = 2 mL/min and waiting when the column is heated up to 50°C, switching of valve was to inject blue dextran at volume of 0.5 ml and then turned back to eluent feeding. Three similar injections were performed with interval 15 minutes.

The data was written in text file and then analyzed by the Microsoft Excel, where the plot was received (see Fig. 2.9).

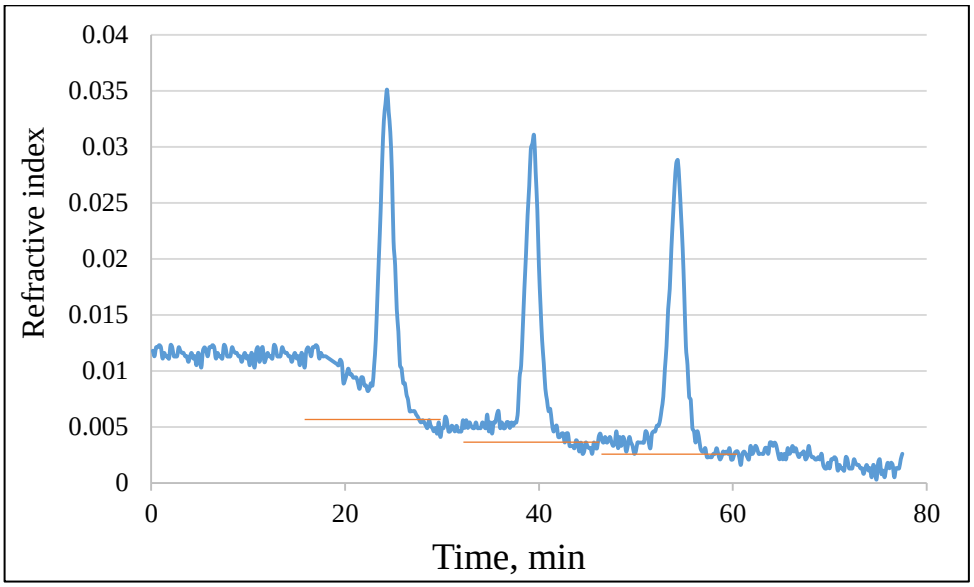

Figure 2.9. The resulting graph of blue dextran detection (each measurement was recorded at 10 seconds interval). The orange solid lines represent the baseline.

The obtained peaks were adjusted to baseline from where the integration of the peak area was made to derive the retention time, t_R, of the tracer. Thereafter, the retention volume was calculated by Eq. 2.7. The injection volume of blue dextran is not negligible compared with elution volume (Gel filtration Principles and Methods, 9-10), therefore its calculation requires subtracting the equipment void volume, V_{RI} = 2.9283 mL, and the half of the injection volume, V_{inj} = 0.5/2=0.25 mL. Then to find porosity the received volume, V_e, is divided by the column volume, V (see Eq. 2.8).

$$V_R = Qt_R \tag{2.7}$$

$$\varepsilon = \frac{V_F}{V} \tag{2.8}$$

The calculation results are presented in Table 2.4. It was found that porosity of the column is equal to 0.3759.

Table 2.4. The experiment results of deriving column porosity

№ of experiment	t_R, min	Q, mL/min	V_R, mL	V_e, mL	ε	Average ε
1	24.3333	2.0032	48.7445	45.5663	0.3764	0.3759
2	24.3333	2.0043	48.7713	45.5930	0.3766	
3	24.1978	2.0050	48.5167	45.3384	0.3745	

2.2.2 Calculation of the isotherm parameters for glucose and fructose

The parameters of the isotherm for single component could be defined by using frontal analysis method, which is widely applied for its simplicity in case of linear behavior of the considered compounds. The feed with different concentrations was prepared for glucose and fructose. It was done for both from 1 g/L to 150 g/L with the following sequence: 1 -> 3 -> 5 -> 10 -> 40 -> 70 -> 110 -> 150 g/L.

Firstly, the glucose component was analyzed. With pumping the large volume at flow rate 2 mL/min, the first feed concentration was injected. The feed with the second concentration was introduced after reaching stable plateau. The refractive index detector was used for compound detection and towards the end of the experiment it was purged to get accurate analyzing. After completing of the experiments with all concentrations, the chromatogram was achieved as it shown in Fig. 2.10.

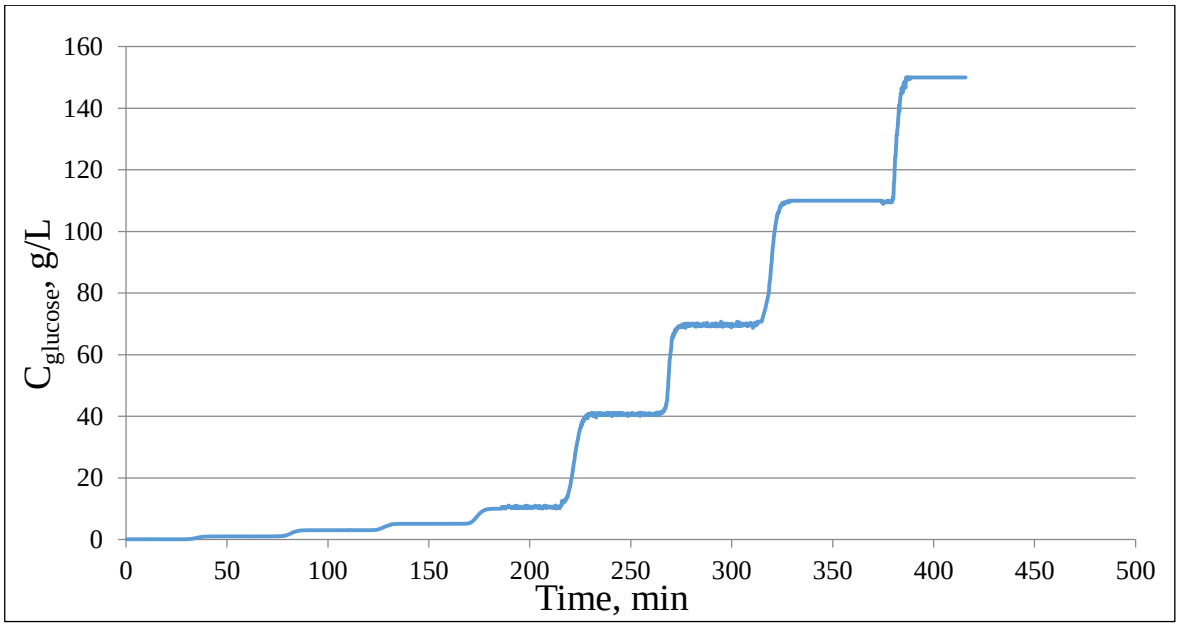

Figure 2.10. The experimental chromatogram obtained by using frontal analysis method to derive glucose isotherm parameters.

Secondly, the experiment with fructose was carried out. The column was washed by the eluent and then ready to further procedures.

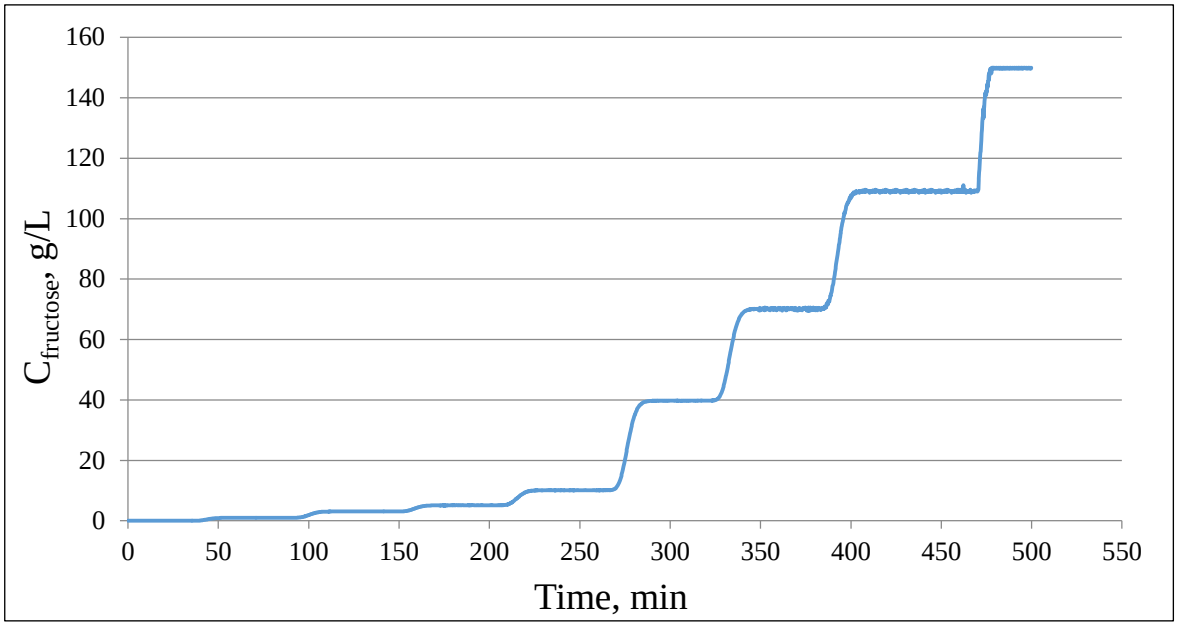

Figure 2.11. The chromatogram obtained by frontal analysis method to determine fructose isotherm parameters.

After getting the plateau, the height of the column was measured to obtain current column volume.

From the obtained data the retention time of the breakthrough curve for investigated concentration of the component could be calculated by integrating the hatched area, left and ride sides of which are equal, and finding the inflection point (see Fig. 2.12). The plateau characterizes the peak concentration which is equivalent to the initial concentration of the prepared solution.

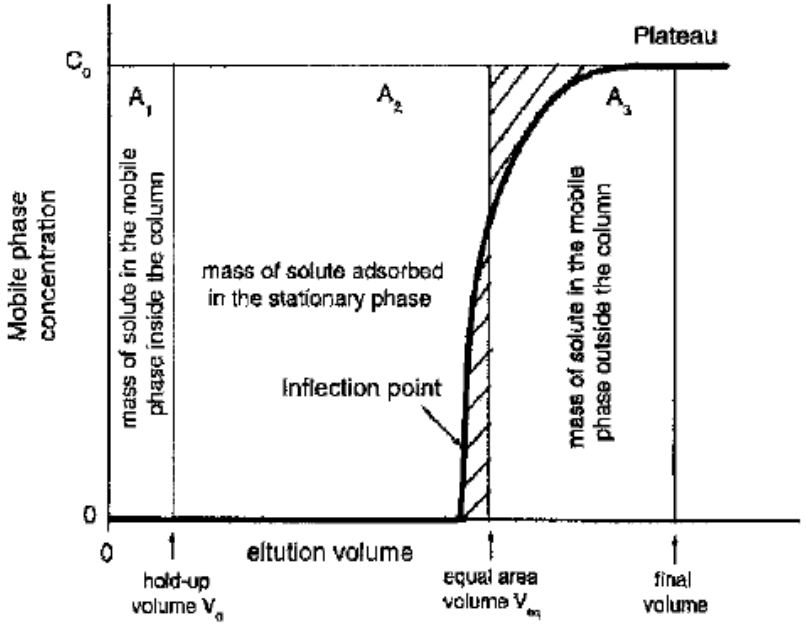

Figure 2.12. Determination of the retention volume (Guiochon et al. 2006, 124).

Thereafter, with analogues steps as for blue dextran, the retention volumes were calculated. It should be noticed that because of using the large solution volume, the elution volume was calculated by subtracting only the equipment void volume. The obtained results reported in the Table 2.5 and Table 2.6.

Table 2.5. The experiment results for glucose separation.

The concentration of glucose, g/L	Q, mL/min	t_R, min	V_R, mL	V_F, mL
1	2.00	36.14	72.4173	69.4891
3	2.01	35.63	71.5379	68.6097
5	2.01	35.71	71.9592	69.0310
10	2.00	35.51	71.1372	68.2089
40	1.99	36.23	72.3549	69.4267
70	2.02	37.40	75.4582	72.5299
110	1.97	36.18	71.3904	68.4621
150	2.10	36.50	76.7339	73.8057

Table 2.6. The experiment results for fructose separation.

The concentration of fructose, g/L	Q, mL/min	t_R, min	V_R, mL	V_F, mL
1	1.99	45.519	90.4690	87.5408
3	2.01	43.757	87.9734	85.0452
5	1.99	44.007	87.9480	85.0197
10	2.03	43.882	88.9225	85.9942
40	2.00	43.693	87.5870	84.6587
70	2.02	43.489	87.8043	84.8760
110	1.99	43.385	86.5140	83.5858
150	2.02	42.885	86.7564	83.8281

The next step is deriving the Henry constant for glucose. First, the adsorbed amount of compound is calculated by using the following equation (Guiochon et al. 2006, 124):

$$q_{i+1} = q_i + \frac{(C_{i+1} - C_i)(V_{F,i+1} - V_0)}{V_a} \tag{2.9}$$

where $V_0 = V\varepsilon$ is the column void volume, mL, and $V_a = (1-\varepsilon)V$ is the volume of adsorbent in the column, mL.

After obtaining the component concentrations in the adsorbent *q* for all concentrations *C*, the linear isotherms were plotted and the Henry constants were defined after linearization. The corresponding data and graphs are shown below.

Table 2.7. The data for the isotherm construction.

The concentrations for glucose		The concentrations for fructose	
C, g/L	*q*, g/L	*C*, g/L	*q*, g/L
1	0.3043	1	0.5952
3	0.8900	3	1.7196
5	1.4866	5	2.8433
10	2.9246	10	5.7171
40	12.0292	40	22.4296
70	22.3893	70	39.2284
110	34.0769	110	60.9436
150	48.7805	150	82.7872

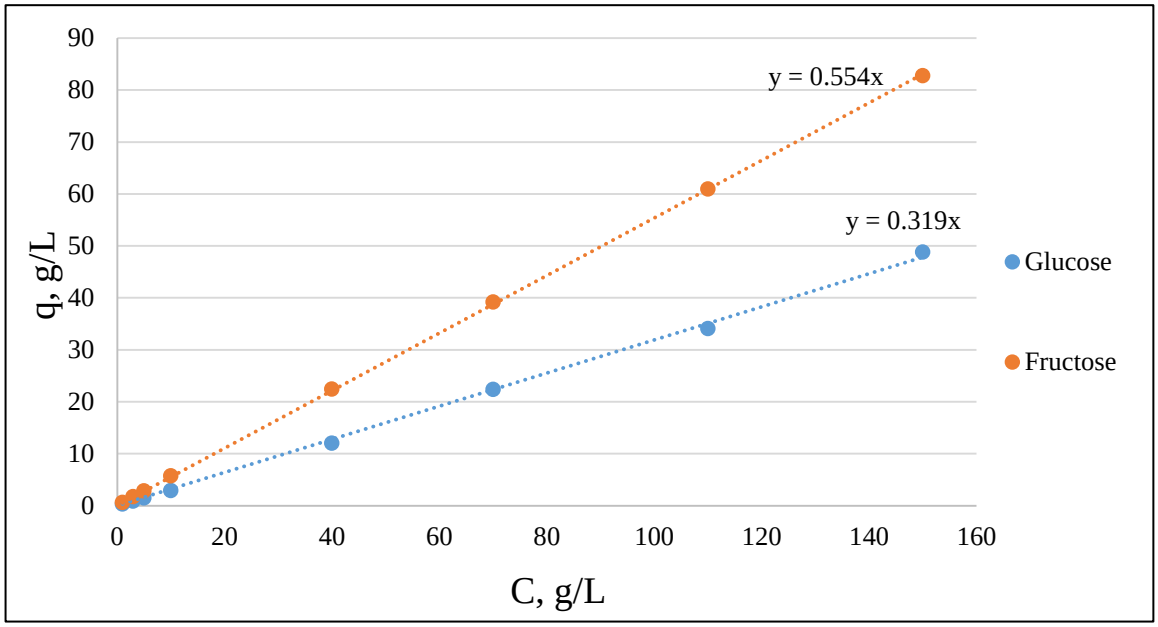

Figure 2.13. The linear isotherms for glucose and fructose. R-squared value for fructose is 0.9999 and for glucose is 0.9989.

The obtained the Henry constants for glucose (H=0.32) and for fructose (H=0.55) would be used for further investigations.

2.2.3 NTP measurements of the experimental column

Defining column efficiency includes 4 experiments for separate solutions of glucose and fructose. The injected amount was established as 3% of the column volume or 3.6 mL. The injection of the one concentration was done twice with 30 minute interval for the flow rate 2 mL/min and 20 minute - for 4 mL/min. The concentration of the both components was 5 g/L.

The first experiment was performed with 5 g/L glucose solution. As it could be seen from the Fig. 2.14, the obtained chromatogram corresponds to Gaussian peak and NTP could be defined from the data by finding the peak center of mass.

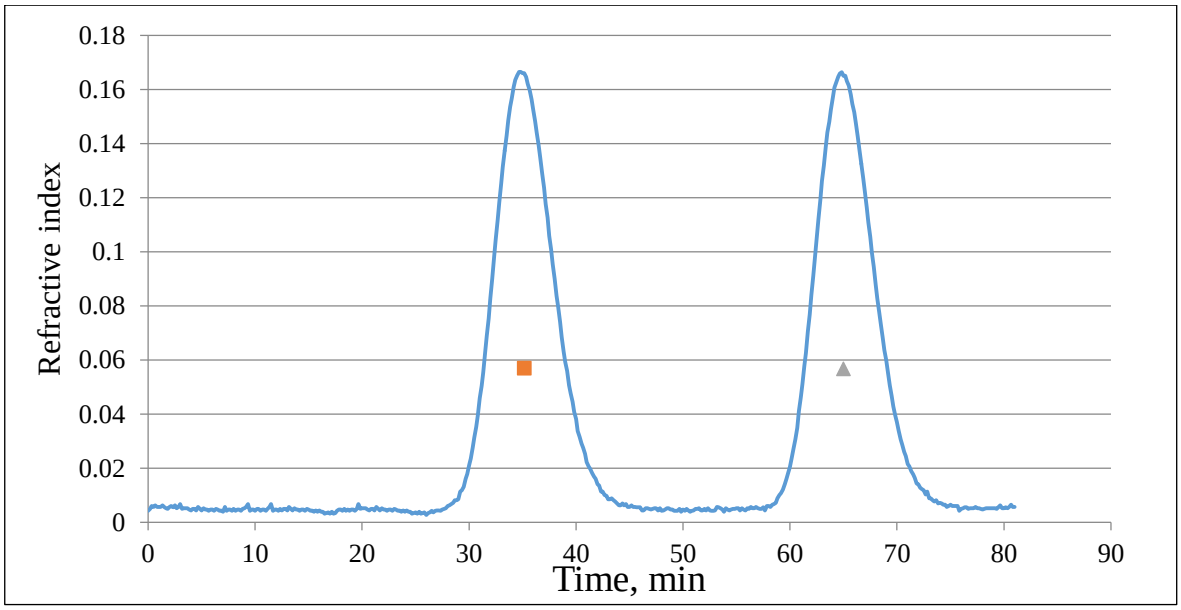

Figure 2.14. The experimental chromatogram for glucose, where first point (■) represents the calculated center of mass of the first peak and second (▲) - the center of mass of the last peak.

The center of mass was derived by integration the profile area with using Microsoft Excel, and then checked by MATLAB code. The efficiency of the column was found by using Eq. 2.2 and the final results are presented in the table below.

Table 2.8. The results of data processing for NTP determination for glucose separation.

№ of injection	C, g/L	t_R, min	V_R, mL	V_F, mL	Q, mL/min	NTP
1	5	35.3628	71.3020	66.5738	2.0163	125.61
2		35.1561	70.7692	66.0410	2.0130	131.71
3		17.6961	71.0586	66.3303	4.0155	64.27
4		17.6991	71.0336	66.3053	4.0134	70.95

After finishing with the laboratory work with glucose, the column was flushed and then similarly experiments were conducted for the second component – fructose.

Table 2.9. The results of data processing for NTP determination for fructose separation.

№ of injection	C, g/L	t_R, min	V_R, mL	V_F, mL	Q, mL/min	NTP
1	5	44.2206	89.0956	84.3674	2.0148	100.02
2		44.2427	88.8393	84.1110	2.0080	98.54
3		22.0700	88.4166	83.6884	4.0062	56.51
4		21.9310	87.8402	83.1120	4.0053	55.53

Since we know the NTP values for laboratory column, which is packed with Finex CS11GC in Ca^{2+} form resin, the simulations could be performed in MATLAB to obtain the

same *N*. It would help to understand what is the maximum purity can be achieved with this column to get the region of operating parameters as for ideal conditions and then check this hypothesis in practical implementation.

Another case is to test obtained the Henry constants for their suitability for modeling. It was checked in the same MATLAB code, as it was done at the first part of batch simulations, but for single component only. The parameters were set to practical values which were used in four previous experiments. The situation was similar to each simulation, therefore, only one would be shown in detail view.

After the overlay of graphs the time of the fronting and tailing of the peaks matches (see Fig. 2.15) and also the practically identic retention volumes were obtained. The same was for other cases. It allows saying that further simulations can be done and they would be close to real.

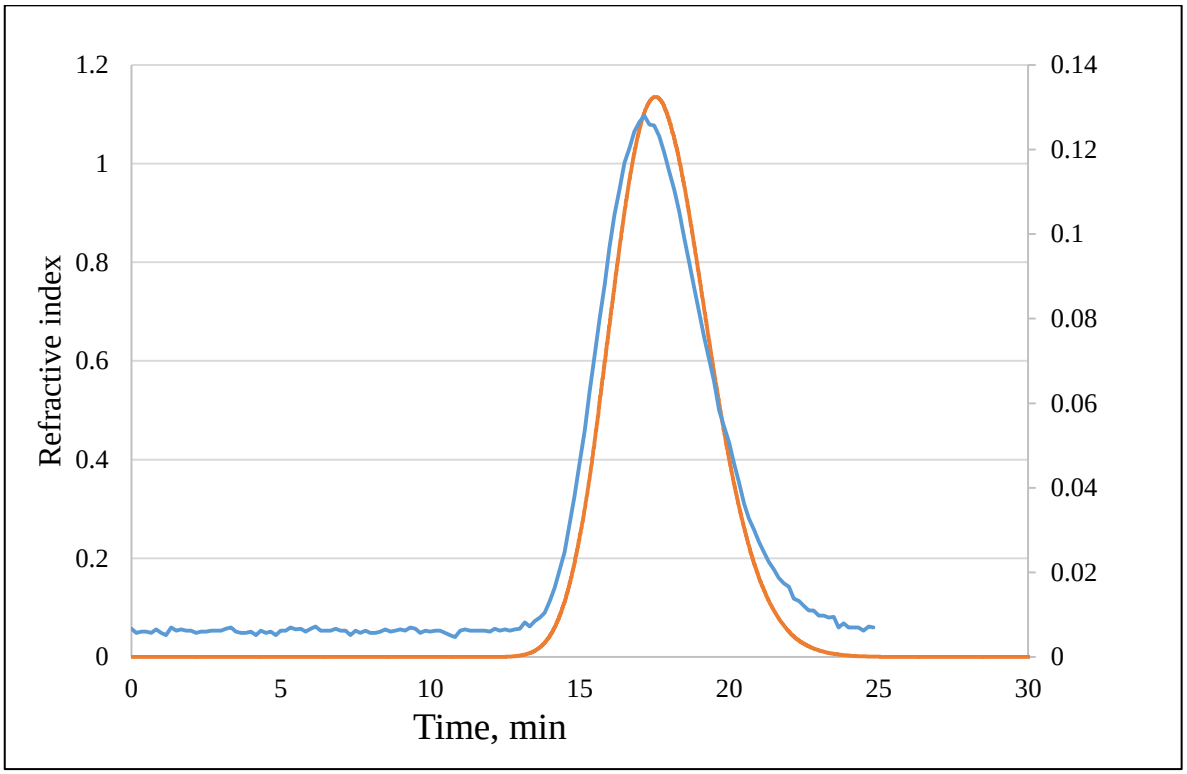

Figure 2.15. Overlaying two chromatograms of glucose separation at 4 mL/min. The blue solid line is experimental chromatogram and the orange solid line is modeled chromatogram with appropriate parameters.

2.3 Estimation of the minimum NTP for Finex CS11GC gel type resin and comparison with Dowex Monosphere 99/Ca

The further simulations were continued with the aim to find minimum number of theoretical plates with corresponding isotherm parameters. The constant parameters are presented in Table 2.10. It is worth noting that these parameters were chosen the same as for the first simulations to obtain comparable results.

Table 2.10. The constant parameters of the simulation.

The name of parameter	The value of parameter	
The column parameters		
Height, m	0.7	
Diameter, m	0.015	
Volume, ml (V)	120	
Bed porosity (ε)	0.4	
Flow rate, mL/min (Q)	4	
The component parameters		
	Glucose (A)	Fructose (B)
The concentration, g/L	116	84
The Henry constant	0.32	0.55

The sets of the simulations were performed with new isotherm parameters at different column efficiency. The first part relates to the region with 80% purity of both components (see Fig. 2.16), where minimum N = 650 was determined.

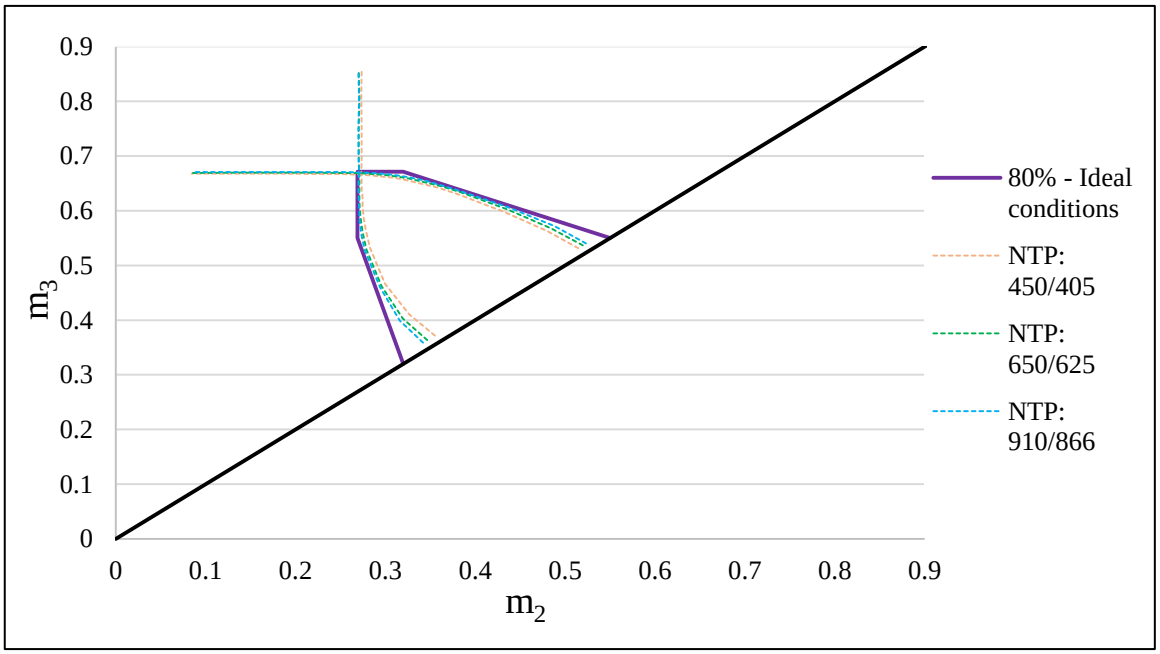

Figure 2.16. The results of simulations for obtaining boundaries of the operating regions at different NTP level. Purity for both components is set to 80%. The particle size varied from $280 \cdot 10^{-6}$ m to $150 \cdot 10^{-6}$ m and the intraparticle diffusion coefficient, D_{pore}, is $1 \cdot 10^{-8}$ m^2/s.

The second part is devoted to higher purity constraint – 90%. For this requirement the minimum NTP was found at 2700 (see Fig. 2.17).

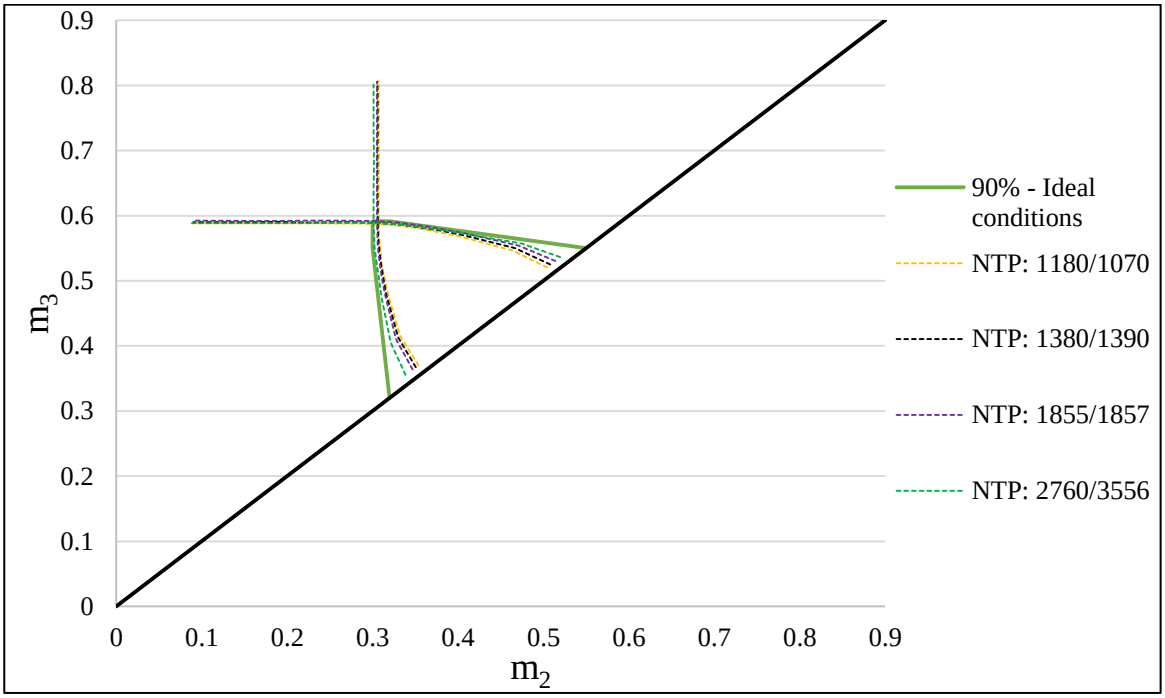

Figure 2.17. The changing of the area of operating parameter space from increasing number of theoretical plates in the column. The separated products have 90% purity. The intraparticle diffusion coefficient, D_{pore}, is equal to $1 \cdot 10^{-8}$ m^2/s and the diameter of the particle gradually decreased up to $50 \cdot 10^{-6}$ m.

The third part contains the investigation for 99.9% purity requirement for both compounds. As it is shown on Figure 2.18, the highest *N* value, which could be reached in the program, cannot satisfy the region with 100% purity at ideal conditions, therefore, it requires the NTP more than 10 000 that could be performed only in analytical scale chromatography. However, by reducing purity to 98.5-98%, 9 000 becomes quite suitable to reach “ideal” region.

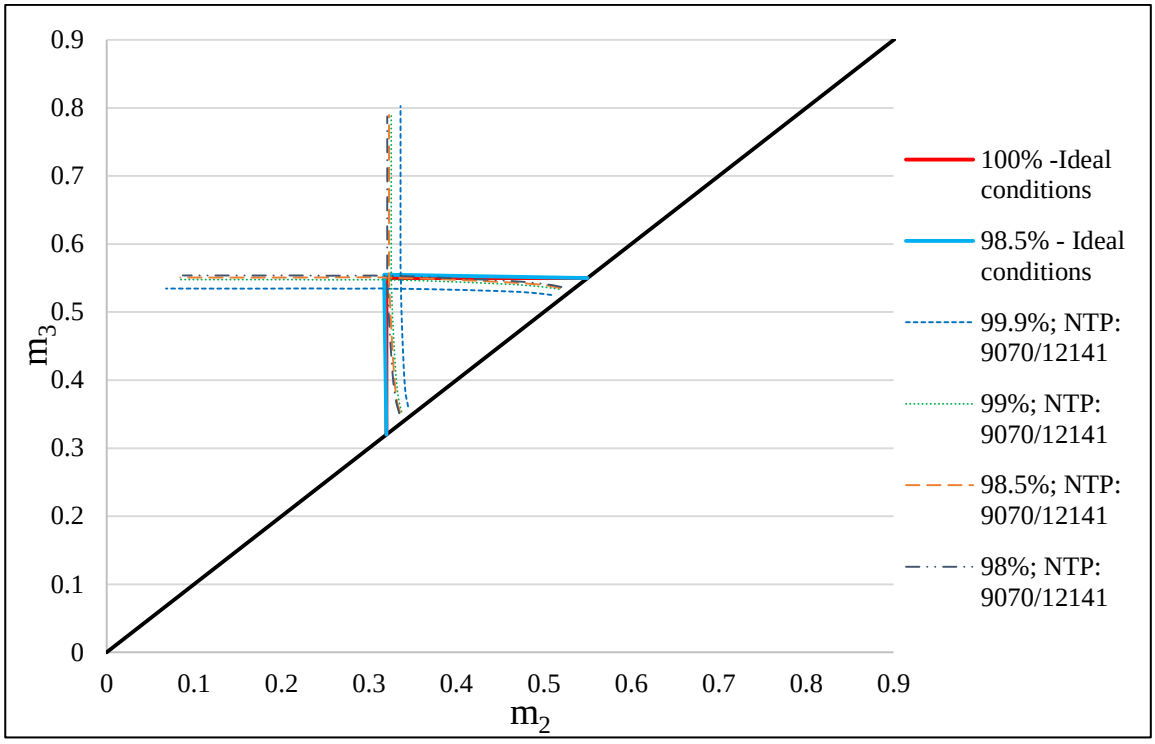

Figure 2.18. Influence of column efficiency on operating parameter space. The target purity of the both products was set from 99.9% to 98%.

Comparison of the requirements for target purity with different resins and, hence the Henry constants of the linear isotherm, is presented below.

Table 2.11. The results of calculation the minimum number of theoretical plates.

The name of parameter	The value of parameter
Dowex Monosphere 99/Ca gel type resin: H= 0.29 (glucose) and H=0.63 (fructose)	
80% purity	≥ 300
90% purity	≥ 900
99% purity	≥ 9 000
Finex CS11GC gel type resin in Ca^{2+} form: H= 0.32 (glucose) and H=0.55 (fructose)	
80% purity	≥ 650
90% purity	≥ 2 700
98.5% purity	≥ 9 000

From the table above it could be seen that for new isotherm parameters it is required more than 2 times higher number of theoretical plates due to the lower selectivity and differing physical property of the used adsorbent. In addition, for both cases to get 100% purity of the components the NTP should be approximately higher than 10 000, but with decreasing purity to 99% and to 98.5% with constants 0.29/0.63 and 0.32/0.55, respectively, the region could be covered at lower column efficiency.

2.4 Simulation of SSR chromatography for glucose and fructose separation

To estimate the possibility and the advantages of applying SSR chromatography (see Chapter 1, Section 1.5) with considered isotherm parameters the simulations were performed in the same MATLAB code. The runmode was changed to "SSR" and the cut times for glucose and fructose were taken from the previous batch simulations at higher injection volumes.

For comparison of the batch and SSR chromatography the factors such as relative productivity and eluent consumption were applied (see Chapter 1, Section 1.1.3). The first means the ratio of the current productivity of SSR, PR_{SSRi}, to maximum productivity of the batch chromatography, PR_{batch}. Therefore, it is necessary to find PR_{batch} (or the highest injection volume), which is expressed by point of the single cut time where same purity for both components is realized. The second factor could be derived in the same way but for the eluent consumption (EC). The example of the comparing is presented below.

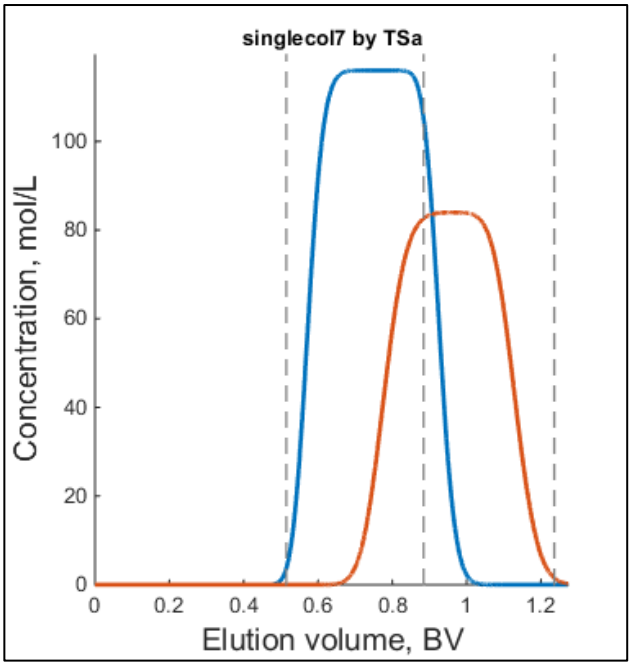

Figure 2.19. The batch chromatographic separation profile with single cut time. V_{inj} = 43.74 mL. H = 0.29 (glucose) and H = 0.63 (fructose). Purity is set to 80%. N = 300.

The maximum productivity was found firstly for the batch separation (see Table 2.12).

Table 2.12. The productivity and eluent consumption for batch mode

The injection volume, mL	PR_{batch}, g/L(bed)/h		EC_{batch}, L(eluent)/g	
	Glucose	Fructose	Glucose	Fructose
43.74	96.4025	55.7319	0.01026	0.01774

The next step is devoted to SSR chromatography. The obtained results from the simulations are shown in Table 2.13. The values of the compare parameters were written after setting steady state condition.

Table 2.13. The productivity and eluent consumption for SSR mode

The injection volume, mL	PR_{SSR}, g/L(bed)/h		EC_{SSR}, L(eluent)/g		Fresh feed, mL	Compound purity, %	
	Glucose	Fructose	Glucose	Fructose		Glucose	Fructose
45.77	94.4676	54.5238	0.0102	0.0177	43.8024	79.97	80.08
48.24	92.1072	53.2008	0.0102	0.0177	43.8432	79.96	80.02
50.72	89.8654	51.8537	0.0102	0.0177	43.8172	79.96	80.11
53.19	87.5123	50.5425	0.0102	0.0177	43.7912	79.98	80.11
55.67	85.4262	49.3413	0.0102	0.0177	43.7984	79.95	80.10

The Fig. 2.20 represents the peak profile of the sixth cycle on the left side and overlaid chromatograms from 1 to 6 cycles on the right side. The number of cycles means the value required for establishment of steady state condition – in last three cycles the feed concentration has not changed. The dotted line indicates from left to right: the beginning and the end of collection of the glucose, and the beginning and the end of fructose collection.

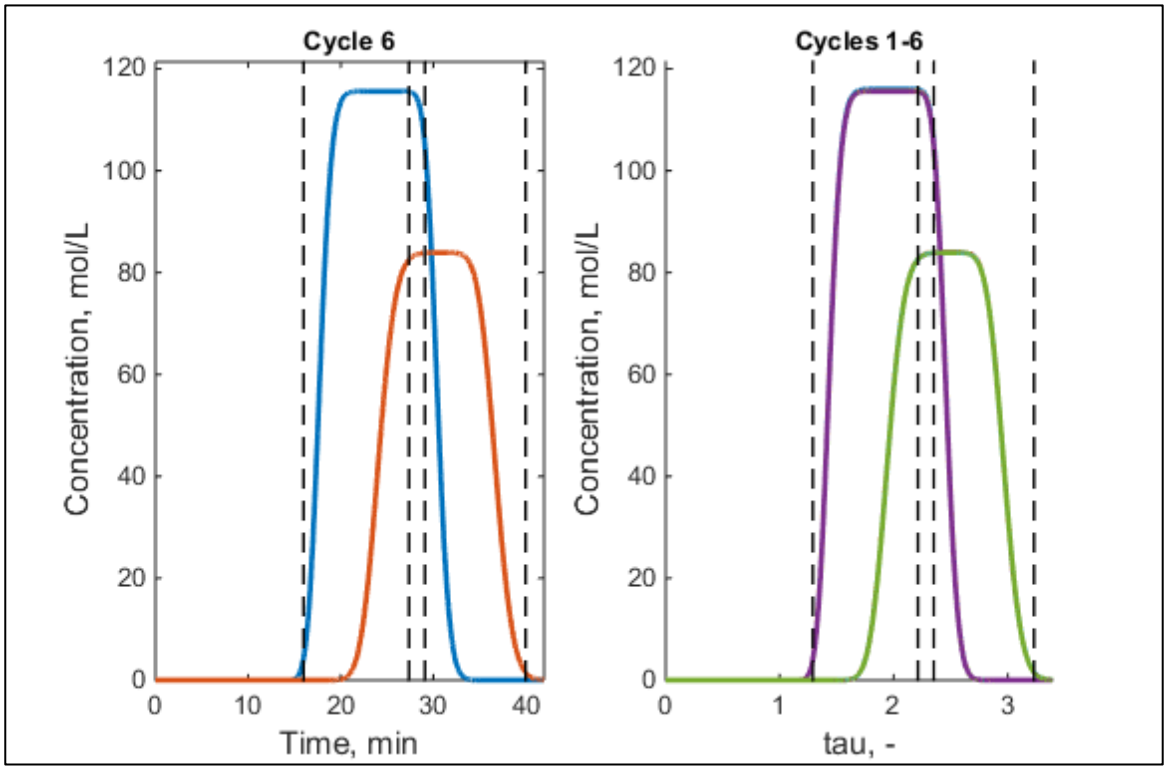

Figure 2.20. The separation profiles for SSR chromatography with V_{inj} = 50.72 mL. H = 0.29 (glucose) and H = 0.63 (fructose). Purity is set to 80%. N = 300.

To illustrate the results of the relative productivity and eluent consumption calculation the data was combined in one graph (see Fig. 2.21).

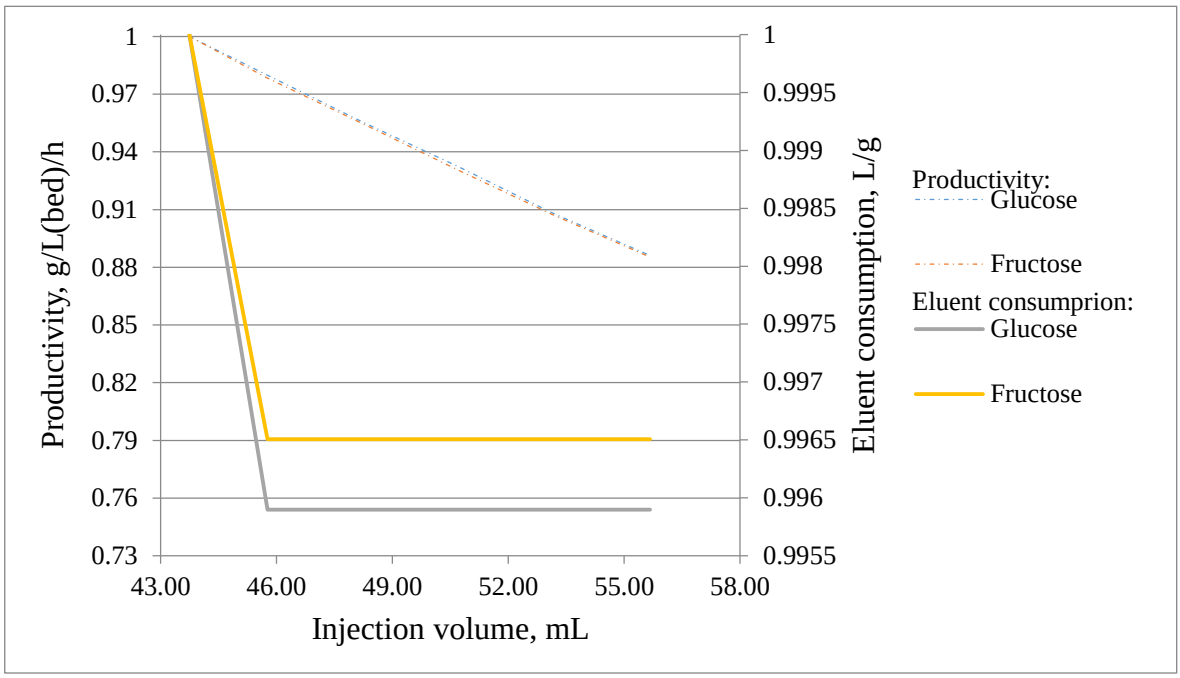

Figure 2.21. The dependence of relative *PR* and *EC* from injection volume, which is ranged from 35.36 mL to 55.67 mL.

The figure shows that *PR* and *EC* are decreasing with the operation at high injection volume. The reduction of the eluent consumption stops at some value because of the reaching the steady state. However, the productivity of SSR in comparison with batch is constantly decreasing. It could be explained by the fact that operating in SSR mode is carrying out at high column loading and the plateau region is appeared (see Fig. 2.22). The cut times are crossing this region and, thus, recycling feed may contain high enough amount of fresh feed, what affects the final volume of the product (becomes less) and the composition of recycling fraction itself.

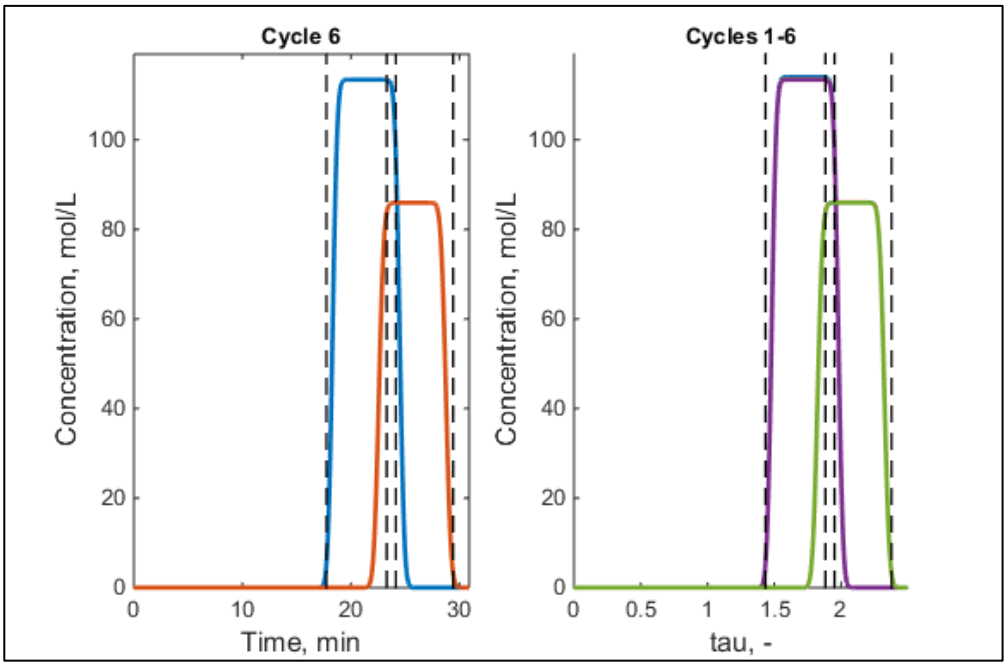

Figure 2.22. The chromatograms for SSR chromatography with V_{inj} = 24.74 mL (90% purity, N=2700, H=0.32 (glucose) and H=0.55 (fructose)).

The simulations with SSR were performed for all other experiments considered range of NTP and for the Henry constants obtained for laboratory column with packed resin. From them it was received the analogous results. It means that the obtained operating parameters are fully applicable for designing of SSR chromatography from batch, because purity of the components corresponds to the desired. Nevertheless, the productivity of SSR should be higher (Yan and Orihuela 2007, 225 and Yan et al. 2008, 144). This is related to the fact that the comparison was made only with constant NTP both for batch and for SSR. To increase *PR*, the SSR process should be optimized (Heinonen, Niskakoski and Sainio 2016, 265-271). It could be done with decreasing *N*, for example, by changing flow rate to decrease cycle time. In addition, a stronger dispersion of elution profiles would be appeared and batch process with a single cut could not be applied to obtain target purities, so the productivity of SSR would be higher in comparison with batch chromatography.

CONCLUSIONS

The aim of the investigation was to find out the behavior of the operating boundaries at different column efficiency. Therefore, the sets of simulations with using special software were performed. To run the program – the parameters were set for an assumed column volume 120 mL and packed with Dowex Monosphere 99/Ca with the appropriate isotherm parameters. The purity requirements were specified as 80%, 90% and 99.9% for glucose and fructose. The first obtained results showed that with increasing efficiency of the column the area of the region of feasible operating parameters expanding also (see Fig. 2.2 and Fig. 2.4). Moreover, it was established that at some value of NTP the feasible operating parameter space at non-ideal conditions is close to be described by the boundaries of the region under ideal conditions. This fact may be intended to simplify the designing of the batch, SSR or SMB separation process. The required minimum NTP was summarized in Table 2.11.

To compare obtained results, the experiments with real column, which was packed with Finex CS11GC gel type resin in Ca^{2+} form, were carried out. The new isotherm parameters were derived by using frontal analysis method. Also, the column efficiency was defined for a number of flow rates. Similarly, the additional simulations were made for the obtained Henry constants and the minimum NTP was also estimated and given in Table 2.11. It was observed that for new isotherm parameters it is required more than 2 times higher number of theoretical plates. Possibly, it could be related with lower selectivity and differing physical property of the used adsorbent. Moreover, the minimum NTP, which is required to obtain the boundaries as for ideal conditions, is higher than 10 000 for both cases. However, the region could be covered at lower column efficiency if the purity constraints decrease to 99%. It means that the operating in the region with “ideal” boundaries is more profitable for lower purity requirements of the component. Furthermore, knowing the efficiency of the laboratory column and after the designing of the separation model in MATLAB, the validation experiments could be made for batch, SMB (with applying the Unified Design method) and SSR chromatography.

Further simulations were devoted to SSR chromatography with aim to estimate the possibility and the advantages of its applying with the considered Henry constants. The obtained operating parameters from batch chromatography simulations are fully applicable for designing of SSR chromatography. The comparison was made by using the following

factors: relative productivity and eluent consumption. It was found that *PR* and *EC* are decreasing with increasing the injection volume (see Fig. 2.21). The productivity of SSR in comparison with batch is constantly decreasing, instead of the characteristic ascending at first. It could be explained by the fact that operating in SSR mode is carrying out at the plateau region (see Fig. 2.22). Moreover, it should be noticed that the comparison was made at constant NTP both for batch and for SSR, what means that the SSR process was not optimized. The optimization could be done with decreasing *N*, for example, by changing flow rate to decrease cycle time of separation. It would entail a stronger dispersion of elution profiles, where the desired purities could not be obtained with the batch process with a single cut and where the difference in productivity would be higher in favor of SSR.

REFERENCES

Aniceto José P.S. and Silva Carlos M. 2015. Preparative Chromatography: Batch and Continuous. Analytical Separation Science, First Edition. Wiley-VCH Verlag GmbH & Co. KGaA. 1207-1313 pp.

Bertelsen, H., Eriknauer, K., Böttcher, K., Christensen, H., Stougaard, P., Hansen, O. & Jörgensen, F. Process for manufacturing of tagatose, US Patent 6,991,923, 2006.

Camacho-Rubio F. et al. 1995. Kinetic study of fructose-glucose isomerization in a recirculation reactor. The Canadian Journal of Chemical Engineering, Vol. 73. 935-940 pp.

Coelho Mariana S. et al. 2002. Dextran and fructose separation on an SMB continuous chromatographic unit. Biochemical Engineering Journal Vol.12. 215–221 pp.

Cox Geoffrey B. (ed.) 2005. Preparative Enantioselective Chromatography. Blackwell Publishing Ltd. 330 p. ISBN 1-4051-1870-9.

Dow, DOW Technical Manual: Chromatographic Separation of Fructose and Glucose Using Dowex Monosphere 99ca Chromatographic Separation Resin. Form No. 177-01566-0209, 2010.

Forssén Patrik, Samuelsson Jörgen and Fornstedt Torgny. 2014. Relative importance of column and adsorption parameters on the productivity in preparative liquid chromatography II: Investigation of separation systems with competitive Langmuir adsorption isotherms. Journal of Chromatography A, 1347 (2014). 72–79 pp.

Fraser-Reid Bertram O. (ed.), Tatsuta Kuniaki (ed.) and Thiem Joachim (ed.). 2001. Glycoscience: Chemistry and Chemical Biology I-III: with contributions by numerous experts. New York: Springer-Verlag. 2854 p. ISBN 3-540-67764-X.

Ganetsos G. (ed.) and Barker P.E. (ed.). 1992. Preparative and Production Scale Chromatography. New York: Marcel Dekker, Inc.

Gel filtration Principles and Methods. 8th edition. Amersham Pharmacia Biotech. 103 p. ISBN 91-97-0490-2-6.

Gottschalk Uwe (ed.). 2009. Process scale Purification of Antibodies. New Jersey: John Wiley & Sons, Inc. 430 p. ISBN 978-0-470-20962-2.

Gramblicka Michal and Polakovic Milan. 2007. Adsorption Equilibria of Glucose, Fructose, Sucrose, and Fructooligosaccharides on Cation Exchange Resins. J. Chem. Eng. Data 52 (2007). 345-350 pp.

Gritti Fabrice et al. 2003. Determination of single component isotherms and affinity energy distribution by chromatography. Journal of Chromatography A, 988 (2003). 185–203 pp.

Guiochon G. et al. 2006. Fundamentals of Preparative and Nonlinear Chromatography. Felinger A., Shirazi Dean G., Katti Anita M. Second Edition. Sang Diego, USA: Elsevier Inc. 975 p. ISBN-13: 978-0-12-370537-2.

Hartig Dave, Waluga Thomas and Scholl Stephan. 2015. Expanding the elution by characteristic point method to columns with a finite number of theoretical plates. Journal of Chromatography A, 1413 (2015). 77–84 pp.

Heinonen Jari and Sainio Tuomo. 2013. Chromatographic Fractionation of Lignocellulosic Hydrolysates. In Dmitry Yu. Murzin, editor: Advances in Chemical Engineering, Vol. 42, Burlington: Academic Press. 261-349 pp. ISBN: 978-0-12-386505-2.

Heinonen Jari, Niskakoski Henna and Sainio Tuomo. 2016. Chromatographic separation of ethyl-β-D-glucopyranoside and D-glucose with steady-state recycling chromatography. Separation and Purification Technology. Vol. 169. 262–272 pp.

Helfferich , Friedrich G. 1995. Ion Exchange. USA: Dover Publications, Inc.

Helfferich Friedrich G. and Liberti L. (ed.) 1983. Mass Transfer and Kinetics of Ion Exchange. The Hague: Martinus Nijhoff Publishers. 459 p. ISBN-13: 978-94-009-6901-8.

Khosravanipour Mostafazadeh A. et al. 2011. Separation of fructose and glucose from date syrup using resin chromatographic method: Experimental data and mathematical modeling.

Kiselev A. 1986. Mezhmolekulyarnye vzaimodeistviya v adsorbtsii i khromatografii (Intermolecular interactions in adsorption and chromatography). Moscow: High. Sch. 360 p.

Lee Kwang-Nam, Lee Chang-Yong and Lee Won-Kook. 1996. Separation of glucose and fructose using a semi-continuous chromatographic refiner with and without a purge column. Korean Journal of Chemical Engineering, Vol. 13, No. 1. 67-74 pp.

Luz D.A. et al. 2008. Adsorptive separation of fructose and glucose from an agroindustrial waste of cashew industry. Bioresource Technology 99 (2008). 2455–2465 pp.

Masuda Takako et al. 2002. High-performance liquid chromatographic separation of carbohydrates on a stationary phase prepared from polystyrene-based resin and novel amines. Journal of Chromatography A, 961 (2002). 89–96 pp.

Mohamed K. Hadj-Kali and Inas M. AlNashef. 2015. Using Ionic Liquids for the Separation of Carbohydrates. International Journal of Chemical Engineering and Applications, Vol. 6, No. 6, December 2015. 417-421 pp. DOI: 10.7763/IJCEA.2015.V6.521

Moreno-Vilet L. et al. 2014. Assessment of sugars separation from a model carbohydrates solution by nanofiltration using a design of experiments (DoE) methodology. Bonnin-Paris J., Bostyn S., Ruiz-Cabrera M.A., Moscosa-Santillán M. Separation and Purification Technology 131 (2014). 84–93 pp.

Nobrea C. et al. 2009. Comparison of adsorption equilibrium of fructose, glucose and sucrose on potassium gel-type and macroporous sodium ion-exchange resins. Analytica Chimica Acta 654 (2009). 71–76 pp.

Pedruzzi I., Borges da Silva E.A. and Rodrigues A.E. 2008. Selection of resins, equilibrium and sorption kinetics of lactobionic acid, fructose, lactose and sorbitol. Separation and Purification Technology 63 (2008). 600–611 pp.

Rajendran Arvind, Paredes Galatea and Mazzotti Marco. 2009. Simulated moving bed chromatography for the separation of enantiomers. Journal of Chromatography A, 1216 (2009). 709–738 pp.

Raquel Cristine Kuhn, Marcio A. Mazutti and Francisco Maugeri Filho. 2012. Kinetic and mass transfer effects for adsorption of glucose, fructose, sucrose and fructooligosaccharides into X zeolite. LWT - Food Science and Technology 48 (2012). 127-133 pp.

Rathore Anurag S. et al. 2003. Qualification of a Chromatographic Column Why and How to Do It. BioPharm International March 2003. 30-40 pp.

Ribeiro et al. 2006. Binary Mutual Diffusion Coefficients of Aqueous Solutions of Sucrose, Lactose, Glucose, and Fructose in the Temperature Range from (298.15 to 328.15) K. Journal of Chemistry Engineering Data Vol. 51. 1836-1840 pp.

Saari Pia et al. 2010. Study on Industrial Scale Chromatographic Separation Methods of Galactose from Biomass Hydrolysates. Chemical Engineering Technology Vol. 33, No. 1. 137–144 pp.

Saari Pis. 2011. Industrial Scale Chromatographic Separation of Valuable Compounds from Biomass Hydrolysates and Side Streams. Doctoral dissertation for the degree of Doctoral Science. Aalto University, School of Chemical Technology, Department of Biotechnology and Chemical Technology. Aalto University. 64 p. ISBN: 978-952-60-4130-8.

Sainio et al. 2011. Influence of Ion Exchange Resin Particle Size and Size Distribution on Chromatographic Separation in Sweetener Industries. Kärki Ari, Kuisma Jarmo and Mononen Heikki. Ion Exchange and Solvent Extraction. A Series of Advances V. 20. Taylor & Francis Group, LLC. 145-171 pp.

Sakodynskii K.I. et al. 1993. Analiticheskaya khromatografiya (Analytical chromatography). Sakodynskii K.I., Brazhnikov V.V., Volkov S.A., Zel"venskii V.Yu., Gankina E.S., Shatts V.D. Moscow: Khimiya. 464 p. ISBN 5-7245-0136-8.

Schmidt-Traub H. (ed.) 2005. Preparative Chromatography of Fine Chemicals and Pharmaceutical Agents. Weinheim: WILEY-VCH Verlag GmbH & Co. KGaA. 458 p. ISBN: 3-527-30643-9.

Schmidt-Traub Henner (ed.), Schulte Michael (ed.), and Seidel-Morgenstern Andreas (ed.). 2012. Preparative Chromatography. Weinheim, Germany: Wiley-VCH Verlag & Co. 535 p. ISBN: 978-3-527-64931-0

Sheng Peizhu. 1995. Selectivity inverted parametric pumping. Application to the separation of simple sugars. University of Porto. 216 p.

Siitonen Jani and Sainio Tuomo. 2014. Steady state recycling chromatography with solvent removal—Effect of solvent removal constraints on process operation under ideal conditions. Journal of Chromatography A, 1341 (2014). 15–30 pp.

Siitonen Jani and Sainio Tuomo. 2015. Unified design of chromatographic separation processes. Chemical Engineering Science 122 (2015). 436–451 pp.

Siitonen Jani, Sainio Tuomo and Rajendran Arvind. 2013. Design of batch chromatography for separation of binary mixtures under reduced purity requirements. Journal of Chromatography A, 1286 (2013). 55– 68 pp.

Siitonen Jani. 2014. Advanced analysis and design methods for Preparative chromatographic separation processes. Thesis for the degree of Doctor of Science (Technology). Lappeenranta University of Technology, Lappeenranta, Finland. 88 p. ISBN 978-952-265-714-5.

Storti Giuseppe et al. 1993. Robust Design of Binary Countercurrent Adsorption Separation Processes. Mazzotti Marco, Morbidelli Massimo and Card Sergio. AlChE Journal Vol. 39, No. 3. 471-492 pp.

Suvarov et al. 2014. Cycle to cycle adaptive control of simulated moving bed chromatographic separation processes. Kienle Achim, Nobre Clarisse, Guy De Weireld, Alain Vande Wouwer. Journal of Process Control V. 24. 357-367 pp.

The theory of HPLC Band Broadening [on line]. CHROMacademy: <URL: http://www.chromacademy.com/lms/sco3/Theory_Of_HPLC_Band_Broadening.pdf>.

The theory of HPLC Chromatographic parameters [on line]. CHROMacademy: <URL:http://www.chromacademy.com/lms/sco2/Theory_Of_HPLC_Chromatographic_Parameters.pdf>.

Tiihonen Jari et al. 2005. Subcritical water as eluent for chromatographic separation of carbohydrates using cation-exchange resins. Separation and Purification Technology 44 (2005). 166–174 pp.

Tsarev N.I., Tsarev V.I., Katrakov I.B. 2000. Prakticheskaya gazovaya khromatografiya (Practical gas chromatography). Barnaul: Alt. un-t publ. 156 p.

Wang Ya-Jun et al. 2016. Isolation of Fructose from High-Fructose Corn Syrup with Calcium Immobilized Strong Acid Cation Exchanger: Isotherms, Kinetics, and Fixed-

Bed Chromatography Study. The Canadian Journal Of Chemical Engineering Volume 94, March 2016. 537-5465 pp.

Wixom Robert L. (ed.) and Gehrke Charles W. (ed.). 2010. Chromatography A Science of Discovery. New Jersey: Wiley & Sons, Inc. 412 p. ISBN 978-0-470-28345-5.

Xie Yi, Koo Yoon-Mo and Wang Nien-Hwa Linda. 2001. Preparative Chromatographic Separation: Simulated Moving Bed and Modified Chromatography Methods. Biotechnol. Bioprocess Eng. Vol. 6. 363-375 pp.

Yan Tony Q. and Orihuela Carlos. 2007. Rapid and high throughput separation technologies—Steady state recycling and supercritical fluid chromatography for chiral resolution of pharmaceutical intermediates. Journal of Chromatography A, Vol. 1156. 220–227 pp.

Yan Tony Q., Orihuela Carlos and Swanson David. 2008. The Application of Preparative Batch HPLC, Supercritical Fluid Chromatography, Steady-State Recycling, and Simulated Moving Bed for the Resolution of a Racemic Pharmaceutical Intermediate . Wiley InterScience. Chirality 20. 139-146 pp. DOI 10.1002/chir

Zhu Fengmei, Du Bin and Xu Baojun. 2016. A critical review on production and industrial applications of beta-glucans. Food Hydrocolloids 52 (2016). 275-288 pp.

Appendix 1. The simulation results